Current Single Event Effects and Radiation Damage Results for Candidate Spacecraft Electronics

Martha V. O'Bryan[1], *Member, IEEE,* Kenneth A. LaBel[2], *Member, IEEE,*
Ray L. Ladbury[3], *Member, IEEE,* Christian Poivey[4], *Member, IEEE,*
James W. Howard Jr.[5], *Senior Member, IEEE*, Robert A. Reed[2], *Member, IEEE,*
Scott D. Kniffin[3], *Member, IEEE,* Stephen P. Buchner[6], *Member, IEEE,* John P. Bings[7],
Jeff L. Titus[7], *Senior Member, IEEE*, Steven D. Clark[7], *Member, IEEE,*
Thomas L. Turflinger[7], *Member, IEEE*, Christina M. Seidleck[1],
Cheryl J. Marshall[2], *Member, IEEE,* Paul W. Marshall[8], *Member, IEEE,* Hak S. Kim[5],
Donald K. Hawkins[2], Martin A. Carts[1], James D. Forney[5], Michael R. Jones[3], *Member, IEEE,*
Anthony B. Sanders[2], Timothy L. Irwin[6], Stephen R. Cox[2], Zoran A. Kahric[6],
Christopher D. Palor[3], and James A. Sciarini [3]
1. Raytheon Information Technology & Scientific Services, Lanham, MD 20706-4392
2. NASA Goddard Space Flight Center, Code 561.4, Greenbelt, MD 20771
3. Orbital Sciences Corporation, McLean, VA
4. Stinger Ghaffarian Technologies Inc., Greenbelt, MD 20770
5. Jackson & Tull Chartered Engineers, Washington, D. C. 20018
6. QSS Group Inc., Lanham, MD 20706
7. NAVSEA Crane - Surface Warfare Center Division, Crane, IN 47522
8. Consultant

Abstract-- We present data on the vulnerability of a variety of candidate spacecraft electronics to proton and heavy ion induced single event effects, proton-induced damage, and total ionizing dose. Devices tested include optoelectronics, digital, analog, linear bipolar, hybrid devices, Analog-to-Digital Converters (ADCs), Digital-to-Analog Converters (DACs), and DC-DC converters, among others.

I. INTRODUCTION

As spacecraft designers use increasing numbers of commercial and emerging technology devices to meet stringent performance, economic and schedule requirements, ground-based testing of such devices for susceptibility to single event effects (SEE), total ionizing dose (TID), and proton-induced damage has assumed ever greater importance.

The studies discussed here were undertaken to establish the sensitivities of candidate spacecraft electronics to heavy ion and proton-induced single event upsets (SEU), single event latchup (SEL), single event transient (SET), TID and proton damage (ionizing and non-ionizing).

The work presented is sponsored by NASA Electronic Parts and Packaging (NEPP) Program's Electronics Radiation Characterization (ERC) Project, Defense Threat Reduction Agency (DTRA) under IACRO 02-4039I, NASA Remote Exploration and Experimentation (REE) Project and NASA Flight Projects.

M. V. O'Bryan is with Raytheon Information Technology & Scientific Services, Lanham, MD 20706-4392 (telephone: 301-286-1412, e-mail: martha.obryan@gsfc.nasa.gov).

Kenneth A. LaBel is with NASA/GSFC, Code 561, Greenbelt, MD 20771 USA (telephone: 301-286-9936, e-mail: ken.label@gsfc.nasa.gov).

Robert A Reed is with NASA/GSFC, Code 561, Greenbelt, MD 20771 USA, (telephone: 301-286-2153, e-mail: robert.reed@gsfc.nasa.gov).

II. TEST TECHNIQUES AND SETUP

A. Test Facilities

All SEE and proton-induced damage tests were performed between February 2001 and March 2002. Heavy Ion experiments were conducted at the Brookhaven National Laboratories (BNL) Single Event Upset Test Facility (SEUTF) and at Texas A&M University Cyclotron (TAMU). The SEUTF uses a twin Tandem Van De Graaff accelerator while the TAMU facility uses an 88" Cyclotron. Both facilities are suitable for providing a variety of ions over a range of energies for testing. At both facilities, test boards containing the device under test (DUT) were mounted in the test area. For heavy ions, the DUT was irradiated with ions with linear energy transfers (LETs) ranging from 0.59 to 120 MeV•cm^2/mg, with fluences from $1x10^5$ to $1x10^8$ particles/cm^2. Fluxes ranging from $1x10^2$ to $5x10^5$ particles/cm^2 per second, were selected depending on the device sensitivity. Representative ions used are listed in Table I. LETs between the values listed were obtained by changing the angle of incidence of the ion beam on the DUT, thus changing the path length of the ion through the DUT. Energies and LETs available varied slightly from one test date to another.

Proton SEE and damage tests were performed at three facilities: the University of California Davis (UCD) Crocker Nuclear Laboratory (CNL), Tri-University Meson Facility (TRIUMF), and the Indiana University Cyclotron Facility (IUCF). Proton test energies incident on the DUT are listed in Table II. Typically, the DUT was irradiated to a fluence from $1x10^{10}$ to $1x10^{11}$ protons/cm^2, with fluxes on the order of $1x10^8$ protons/cm^2 per second.

The pulsed laser facility at the Naval Research Laboratory was used to generate Single Event Transients (SETs) in integrated circuits. The laser light used had a wavelength of 590 nm that resulted in a skin depth (depth at which the light intensity decreased to 1/e - or about 37% - of its intensity at the surface) of 2 microns.

TID testing was performed using a Co-60 source at the Goddard Space Flight Center Radiation Effects Facility (GSFC REF). The source is capable of delivering a dose rate of up to 0.5 rad(Si)/s, with dosimetry being performed by an ion chamber probe.

TID testing was also performed using a Co-60 source at NAVSEA Crane Naval Surface Warfare Center Division (NAVSEA) Shepherd Model 484 Cobalt-60 Tunnel Irradiator Test Facility. The source is capable of delivering dose rates between 0.8 rad(Si)/sec and 49.5 rad(Si)/sec.

TABLE I: HEAVY ION TEST FACILITIES AND TEST HEAVY IONS

	Ion	Energy, MeV	LET in Si, MeV•cm^2/mg at normal incidence	Range in Si, µm
BNL	C^{12}	102	1.42	193
	O^{16}	131	2.53	145
	F^{19}	145	3.31	126
	Si^{28}	203	7.55	85.3
	Cl^{35}	224	11.1	68.5
	Ti^{48}	253	18.1	53.2
	Ni^{58}	280	26.3	44.3
	Ge^{72}	290	32.7	40.0
	Br^{79}	305	36.9	38.7
	I^{127}	370	60.1	34.3
	Au^{197}	390	84.1	30.2
TAMU	Ne^{20}	298	2.5	331.0
	Ar^{40}	599	7.4	243.7
	Kr^{84}	1260	25.1	154
	Xe^{29}	3282	40.0	250
	Xe^{29}	1935	47.1	127
	* O^{16}	880	0.59	3607
	* Ar^{40}	1980	3.0	1665
	* 55 MeV per nucleon tune			

Table II: Proton Test Facilities and Particles

Facility	Particle	Particle Energy, (MeV)
University of California at Davis (UCD) Crocker Nuclear Laboratory (CNL)	Proton	26.6-63
Tri-University Meson Facility (TRIUMF)	Proton	50-500
Indiana University Cyclotron Facility (IUCF)	Proton	54-197

Table III: Other Test Facilities

Naval Research Laboratory (NRL) Pulsed Laser SEE Test Facility Laser: 590 nm, 3 ps pulse width, beam spot size ~1.5 µm
NAVSEA Crane Naval Surface Warfare Center Division (NAVSEA) Shepherd Model 484 Cobalt-60 Tunnel Irradiator Test Facility
Goddard Space Flight Center Radiation Effects Facility (GSFC REF)

B. Test Method

Unless otherwise noted, all tests were performed at room temperature and with nominal power supply voltages.

1) SEE Testing - Heavy Ion

Depending on the DUT and the test objectives, one or more of three SEE test methods were used:

Dynamic – the DUT was exercised continually while being exposed to the beam. The errors were counted, generally by comparing DUT output to an unirradiated reference device or other expected output. In some cases, the effects of clock speed or device modes were investigated. Results of such tests should be applied with caution because device modes and clock speed can affect SEE results.

Static – the DUT was loaded prior to irradiation; data were retrieved and errors were counted after irradiation.

Biased (SEL only) – the DUT was biased and clocked while I_{CC} (power consumption) was monitored for SEL or other destructive effects. In some SEL tests, functionality was also monitored.

In SEE experiments, DUTs were monitored for soft errors, such as SEUs and for hard errors, such as SEL. Detailed descriptions of the types of errors observed are noted in the individual test results.

SET testing was performed using a high-speed oscilloscope. Individual criteria for SETs are specific to the device being tested. Please see the individual test reports for details. [1]

Heavy ion SEE sensitivity experiments include measurement of the saturation cross sections and the Linear Energy Transfer (LET_{th}) threshold (the minimum LET value necessary to cause an effect at a fluence of $1x10^7$ particles/cm^2).

2) SEE Testing - Proton

Proton SEE tests were performed in a manner similar to heavy ion exposures in many regards. Differences include measuring the SEE cross section as a function of proton energy as opposed to LET, as well as differences in cumulative fluence and particle flux rates.

3) Proton Damage Testing

Proton damage tests were performed on biased devices with functionality and parametrics being measured either continually during irradiation (in-situ) or after step irradiations (for example, every 10 krad(Si), or every $1x10^{10}$ protons).

4) Pulsed Laser Facility Testing

A pulse rate of 100 Hz was chosen. The DUT was mounted on an X-Y stage in front of a 100x lens that produced a spot size of about 1.5 microns. The X-Y stage could be moved in steps of 0.1 micron for accurate

positioning of SEU sensitive regions in front of the focused beam. An illuminator together with a charge coupled device (CCD) camera and monitor were used to image the area of interest, thereby facilitating accurate positioning of the device in the beam. The pulse energy was varied with a neutral density filter and the energy was monitored by splitting off a portion of the beam and directing it at a calibrated energy meter.

5) TID Testing

TID testing was performed to the MIL-STD-883 1019.5 test method [2].

III. Test Results Overview

Abbreviations and conventions are listed in Table IV. Abbreviations for principal investigators (PIs) and test engineers are listed in Table V. Definitions for the categories are listed in Table VI. SEE test results are summarized in Table VII. SEL test results are summarized in Table VIII. Displacement Damage results are summarized in Table IX. TID results are summarized in Table X. Unless otherwise noted, all LETs are in MeV•cm^2/mg and all cross sections are in cm^2/device. This paper is a summary of results. Please note that these test results can depend on operational conditions. Complete test reports are available online at http://radhome.gsfc.nasa.gov [1].

TABLE IV: ABBREVIATIONS AND CONVENTIONS:

H = heavy ion test
P = proton test (SEE)
LET = linear energy transfer (MeV•cm^2/mg)
LET_{th} = linear energy transfer threshold (the minimum LET value for which a given effect is observed for a fluence of $1x10^7$ particles/cm^2 – in MeV•cm^2/mg)
LET_{max} = highest tested LET
LET_{eff} = effective LET (used for angular correction)
SEU = single event upset
SEL = single event latchup
SET = single event transient
SEFI = single event functional interrupt
SEB = single event burnout
BER = bit error rate
BERT = bit error rate tester
DD = displacement damage
< = SEE observed at lowest tested LET
> = No SEE observed at highest tested LET
TID = total ionizing dose
σ = cross section (cm^2/device, unless specified as cm^2/bit)
σ_{SAT} = saturation cross section at LET_{max} (cm^2/device, unless specified as cm^2/bit)
LDC = lot date code
MEMS = Microelectromechanical System
N/A = not available
ACS = Advanced Camera for Surveys
ADC = analog to digital converter
APS = active pixel sensor
ASIC = application specific integrated circuit
CCD = charge coupled device
CTE = charge transfer efficiency
CTI = charge transfer inefficiency
DAC = digital to analog converter
DC/DC Conv. = direct current/direct current converter
DMA = direct memory access
E^2CMOS = electrically erasable complimentary metal oxide semiconductor
EE = electrically erasable
FPR = first pixel response
FWHM = full width half maximum
LDC = lot date code
LED = light emitting diode
LSB = least significant bit
MEMS = Microelectromechanical System
MOSFET = metal-oxide-semiconductor field effect transistor
MSB = most significant bit
NIC = network interface card
OHCI = open host controller interface
PCI = peripheral component interface
PWM = pulse width modulator
SOS = silicon on sapphire
VCSEL = vertical cavity surface emitting laser
V_{DD} = power supply voltage (CMOS)
WFC = Wide Field Camera

TABLE V: LIST OF PRINCIPAL INVESTIGATORS

Abbreviation	Principal Investigator (PI)
JB	John Bings
SB	Steve Buchner
MC	Marty Carts
JF	Jim Forney
JH	Jim Howard
MJ	Mike Jones
HK	Hak Kim
SK	Scott Kniffin
KL	Ken LaBel
RL	Ray Ladbury
CM	Cheryl Marshall
PM	Paul Marshall
CP	Christian Poivey
RR	Robert Reed
AS	Anthony Sanders
CS	Christina Seidleck
JT	Jeff Titus

TABLE VI: LIST OF CATEGORIES

Category	Implications
1	Recommended for usage in all NASA/GSFC spaceflight applications
2	Recommended for usage in NASA/GSFC spaceflight applications, but may require mitigation techniques
3	Recommended for usage in some NASA/GSFC spaceflight applications, but requires extensive mitigation techniques or hard failure recovery mode
4	Not recommended for usage in any NASA/GSFC spaceflight applications

TABLE VII: SUMMARY OF SEE TEST RESULTS

Part Number	Function	LDC	Manufacturer	Particle: (Facility,Date)P.I.	Testing Performed	Summary of Results	Cat.
Op Amps & Analog Comparators:							
LM124	Op Amp	N/A	National Semiconductor	H: (TAMU01MAR) CP Laser: (NRL01MAY) SB/CP/JH	SET	H: SETs observed dependent on conditions [3] Laser: SETs observed. Pulse shape varied with application and bias conditions	2
LM119	Voltage comparator	N/A	National Semiconductor	H: (BNL01DEC) SB Laser: (NRL01MAY) SB/CP/JH	SET	H: SETs observed; LET_{th} and σ_{SAT} dependent on bias conditions [4] [5] Laser: (NRL) SETs observed. Pulse shape varied with application and bias conditions	2
Programmable Devices:							
PALCE22V10	Programmable array logic	0134	Cypress	H: (BNL02MAR) SK	SEL/SET	SEFI $LET_{th} < 7.9$; SEL $LET_{th} < 7.9$	3
ATF22V10B	EE Programmable logic device	0127	Atmel	H: (BNL02MAR) SK	SEL/SET	SEL $LET_{th} > 84.4$; SET $LET_{th} < 11.4$; SET$\sigma = 1x10^{-6}$ at LET 68.9	2
GAL22V10/883	E^2CMOS generic array logic	0043	Lattice	H: (BNL02MAR) SK	SEL/SET	SEL $LET_{th} < 26.6$	3
AN10E40	Analog FPGA	0051	Anadigm	H: (BNL02MAR) SK/AS	SEL/SET	SET $LET_{th} < 11.4$; Loss of configuration $LET_{th} < 11.4$; $18 <$ SEL $LET_{th} < 19.9$	4
Power Devices:							
MDI3051RES05ZF	DC/DC Conv.	0130	Modular Devices Inc.	H: (TAMU01OCT) JH	SET/SEGR/SEB	SET $LET_{th} > 60$. Destructive SEE $LET_{th} <37$ (75% load)	3
MDI3051RED12ZF	DC/DC Conv.	0132	Modular Devices Inc	H: (TAMU01OCT) JH	SET/SEGR/SEB	SET $LET_{th} > 60$. Destructive SEE $LET_{th} <60$ (75% load)	3
MDI3051RED15ZF	DC/DC Conv.	0132	Modular Devices Inc	H: (TAMU01OCT) JH	SET/SEGR/SEB	SET $LET_{th} > 60$. Destructive SEE $LET_{th} <60$ (75% load)	3
LM2651	Switching Regulator	N/A	National Semiconductor	H: (BNL02MAR) CP	SET/SEL	Failure $LET_{th} <25$; $\sigma_{SAT} \sim 2.5 \times 10^{-5}$ at LET 37.5 SET $LET_{th} <5$; SET $\sigma = 1.5x10^{-4}$ at LET 37.5destructive failures observed	3/4
MSK5042	Switching Regulator	0204	MS Kennedy	H: (BNL02MAR) CP/SB	SET/SEB	SEB $LET_{th} < 37$	3/4
LP3470	Voltage Supervisor	0036	National Semiconductor	H: (BNL02MAR) CP/SK	SET	SET $LET_{th} < 1.66$	4
ADCs and DACs::							
AD7714	24 bit ADC	0108; 0041	Analog Devices	H: (BNL01DEC) CP (BNL02MAR) SB	SEE	SEL $LET_{th} \sim 16$; SEL $\sigma = 3x10^{-4}$ at LET of 50; SEU $LET_{th} \sim 4$; $\sigma = 6x10^{-5}$ at LET of 16	3
AD7821	8 bit ADC, 1 MSPS	0034	Analog Devices	H: (TAMU01JUL) CP	SEE	SEL $LET_{th} > 80$; SEU $LET_{th} \sim 4$; $\sigma_{SEU} = 4x10^{-4}$ at LET of 79.6	2
AD9223	12 bit ADC, 3 MSPS	0015	Analog Devices	H: (TAMU01JUL) CP	SEE	$11.4 <$ SEL $LET_{th} < 20$; SEU $LET_{th} \sim 11$	2
LTC1272	12 bit ADC, 250 ksps	0018	Linear Technology	H: (TAMU01JUL) CP	SEE	SEL $LET_{th} \sim 5$; SEL $\sigma = 1x10^{-4}$ at LET of 20; SEU $LET_{th} = 4$	4
LTC1657	16 bit DAC	0105	Linear Technology	H: (BNL02MAR) CP	SEE	SEL $LET_{th} \sim 14$; SEL $\sigma = 6.3x10^{-5}$ at a LET of 37 SEU/SET $LET_{th} \sim 4$; SEU/SET $\sigma = 1.2x10^{-3}$ at a LET of 37	3
ADC1175	8 bit ADC, 20 MSPS	1317	National Semiconductor	H: (BNL02MAR) CP; (TAMU02MAR) CP/JH	SEL(BNL)/ SEU(TAMU)	SEL $LET_{th} \sim 23$; SEL $\sigma = 4.6x10^{-6}$ at LET of 118 SEU/SET $LET_{th} <3$; SEU/SET $\sigma = 4.5x10^{-4}$ at a LET of 49	3

TABLE VII (CONT.): SUMMARY OF SEE TEST RESULTS

Part Number	Function	LDC	Manuf.	Particle: (Facility,Date)P.I.	Testing Performed	Summary of Results	Cat.
Communication Devices:							
TSB12LV26PZT	Link 1394 FireWire OHCI Chipset	CA-OAA 045T	TI	H: (BNL01AUG) PM; (TAMU01OCT) SB/PM/KL P: (TRIUMF01JUL) SB/CS	SEU/SEFI/SEL	H: SEU and SEFI sensitivity depends on the operational conditions [6] P: SEFI Hard Errors $\sigma = 1.48 \times 10^{-10}$ at 105 MeV	3
TSB41AB3PFP	Physical 1394 FireWire OHCI Chipset	OCC 4RTT	TI	H: (BNL01AUG) PM; (TAMU01OCT) SB/PM/KL P: (TRIUMF01JUL) SB/CS	SEU/SEFI/SEL	H: SEFI sensitivity depends on the operational conditions [6] P: SEFI Hard Errors $\sigma = 5.98 \times 10^{-11}$ at 105 MeV	3
CS4210VJG	Link 1394 FireWire OHCI Chipset	VS052 ABC4	National Semiconductor	H: (BNL01AUG) PM P: (TRIUMF01JUL) SB/CS	SEFI/SEL	H: SEL LET <27 P: SEFI Hard Errors $\sigma = 2.56 \times 10^{-10}$ at 105 MeV	4
CS4103VHG	Physical 1394 FireWire OHCI Chipset	VS052 ABC4	National Semiconductor	H: (BNL01AUG) PM P: (TRIUMF01JUL) SB/CS	SEFI/SEL	H: SEL LET <27 P: SEFI Hard Errors $\sigma = 1.46 \times 10^{-10}$ at 105 MeV	4
M3-SW16-8S	16 Port Myrinet Crossbar Switch MYRI2K	84312 87091	Myricom	P: (UCD01OCT) JH/MC	SEE	SEFI σ ~5×10^{-13} cm^2/switch at 63 MeV to 3×10^{12} p/cm^2 SEU Single Packet ~2-9×10^{-13} cm^2/switch; Multi Packet ~3×10^{-13} cm^2/switch No destructive latchups observed [7]	3
Lanai9	Myrinet NIC Protocol Processor MYRI2K	0118	Myricom	P: (UCD01OCT) JH/MC	SEE	SEU $\sigma = 7 \times 10^{-12}$; SEFI $\sigma = 1 \times 10^{-11}$ at 63 MeV to 4.4×10^{11} p/cm^2 No destructive latchups observed [7]	3
SerDeSer	Myrinet Serializer-Deserializer MYRI2K	0123	Myricom	P: (UCD01OCT) JH/MC	SEE	SEU $\sigma = 1 \times 10^{-11}$; SEFI $\sigma = 5 \times 10^{-12}$ at 63 MeV to 4×10^{11} p/cm^2 No destructive latchups observed [7]	3
PCIDMA	Myrinet PCI to DMA	0126	Myricom	P: (UCD01OCT) JH/MC	SEE	SEU $\sigma = 3 \times 10^{-12}$; SEFI $\sigma = 1 \times 10^{-11}$ at 63 MeV to 3.4×10^{11} p/cm^2 No destructive latchups observed [7]	3
VCS7146RH	Myrinet Transceiver MYRI2K	0113	Vitesse	P: (UCD01OCT) JH/MC	SEE	SEU $\sigma = 4 \times 10^{-10}$; SEFI $\sigma = 8 \times 10^{-12}$ at 63 MeV to 3.8×10^{11} p/cm^2 No destructive latchups observed [7]	3
K7N803601M	SRAM (in Myrinet System)	0112	Samsung	P: (UCD01OCT) JH/MC	SEE	SEU $\sigma = 9 \times 10^{-11}$; SEFI $\sigma = 1 \times 10^{-11}$ at 63 MeV to 6.8×10^{10} p/cm^2 No destructive latchups observed [7]	3
AD8151	Crossbar Switch	LA 1148.4	Analog Devices	H: (TAMU02MAR) SB/JH P: (UCD02JAN) SB/PM/RR	SEE (also see DD table) P: DD/TID	H: SEL $LET_{th} > 60$; BER $LET_{th} < 2.8$ BER depends on data rate and LET σ_{SAT} depends on operating conditions P: No SELs observed at 63 MeV protons to 1.25×10^{12} p/cm^2; BER depends on data rate	3

TABLE VII (CONT.): SUMMARY OF SEE TEST RESULTS

Part Number	Function	LDC	Manuf.	Particle: (Facility,Date)P.I.	Testing Performed	Summary of Results	Cat.
Miscellaneous:							
LSP2916	High Voltage Driver (MEMS)	0134 0140	Agere Systems	H: (BNL01DEC) SK	SEE	SEL LET_{th} < 26; SEU LET_{th} >26	4
Photobit APS	APS	N/A	Photobit	H: (TAMU01MAR) CM/PM/RR	SEU/SEL	SEL LET_{th} > 106, SETs observed [8]	2/3
Test Sample	5HP SiGe Prescaler	N/A	IBM	H: (TAMU01MAR)RR P: (UCD01MAR) RR	SEU	H: At LET = 0.6; $\sigma = 1x10^{-6}$; $LET_{MAX} = 30$; $\sigma = 7x10^{-6}$; these results are typical and can depend on operational conditions P: $\sigma = 3x10^{-12}$at 63MeV protons; these results are typical and can depend on operational conditions [9].	2/3
PE9301	SOS Prescaler	N/A	Peregrine	H: (TAMU01JUL) RR P: (UCD01MAR) RR	SEU	H: SEU sensitivity depends on operational conditions [10] P: SEU sensitivity depends on operational conditions [10]	2/3
MTX8501	Transmitter	A1312-12	Emcore	P: (UCD02FEB) SB/PM/RR	SET	No SETs observed for 63MeV protons	1
MRX8501	Receiver	A1235-01	Emcore	P: (UCD02FEB) SB/PM/RR	SET	SETs observed for 63MeV protons; varies with application and angle	2
Processors:							
Pentium PIII 1200 MHz	Processor	S-spec: SL5EM	Intel	P: (IU02FEB) JH	SEL/SEU/ SEFI	H: SEL LET_{th} > 15 ; SEU/SEFI LET_{th} <0.7 P: No SEL up to 5.0 x 10^{10} protons/cm^2; SEU/SEFIs observed 195 MeV protons; SEU/SEFI results vary with software test being performed	3
Pentium PIII 1000 MHz	Processor	S-spec: SL4MF SL5DE	Intel	H: (TAMU01MAR & OCT) JH/KL P: (IU01MAY) JH (IU02FEB) JH	SEL/SEU/ SEFI	H: SEL LET_{th} > 15 ; SEU/SEFI LET_{th} <0.7 P: No SEL up to 5.0 x 10^{10} protons/cm^2; SEU/SEFIs observed 195 MeV protons; SEU/SEFI results vary with software test being performed	3
Pentium PIII 933 MHz	Processor	S-spec: SL4KK SL47Q SL4ME SL5DW	Intel	H: (TAMU01MAR & OCT) JH/KL P: (IU01MAY) JH (IU02FEB) JH	SEL/SEU/ SEFI	H: SEL LET_{th} > 15 ; SEU/SEFI LET_{th} <0.7 P: No SEL up to 5.0 x 10^{10} protons/cm^2; SEU/SEFIs observed 195 MeV protons; SEU/SEFI results vary with software test being performed	3
Pentium PIII 850 MHz	Processor	S-spec: SL47M	Intel	P: (IU01MAY) JH	SEL/SEU/ SEFI	P: No SEL up to 5.0 x 10^{10} protons/cm^2; SEU/SEFIs observed 195 MeV protons; SEU/SEFI results vary with software test being performed	3
Pentium PIII 800 MHz	Processor	S-spec: SL457	Intel	H: (TAMU01MAR) JH/KL	SEL/SEU/ SEFI	H: SEL LET_{th} > 15; SEU/SEFI LET_{th} <0.7; SEU/SEFI results vary with software test being performed	3

TABLE VIII: SUMMARY OF SEL TEST RESULTS*

Part Number	Function	LDC	Manuf.	Particle: (Facility,Date)P.I.	Testing Performed	Summary of Results	Cat.
ADCs:							
LTC1604	16 bit ADC, 333ksps	N/A	Linear Technology	H: (TAMU01JUL) CP (TAMU01AUG) CP	SEL	SEL $LET_{th} > 65$	2
LTC1605	16 bit ADC, 100 ksps	9914	Linear Technology	H: (TAMU01OCT) CP/JH	SEL	SEL $LET_{th} < 53$; SEL $\sigma > 1x10^{-2}$ Non destructive	3
LTC1608	16 bit ADC	0120	Linear Technology	H: (BNL02MAR) CP/SK	SEL	SEL $LET_{th} < 87$; $\sigma_{SAT} = 2.5x10^{-7}$ at LET of 94	3
Miscellaneous:							
ADG452	Analog Switch; SOIC 16	0129	Analog Devices	H: (BNL01DEC) CP	SEL	SEL $LET_{th} > 82$	1
ICL7662	Voltage converter; CAN 8	0135	Intersil	H: (BNL01DEC) CP	SEL	SEL $LET_{th} > 82$	1
XA1	ASIC	00(bulk) 01(epi)	AMS CMOS	H: (TAMU01MAR) RL	SEL	1.2 µm Bulk Silicon: $4 < LET_{th} < 5$; $\sigma \sim 1x10^{-2}$ at LET of 40 0.8 µm epi Silicon: $6 < LET_{th} < 8$; $\sigma \sim 1x10^{-3}$ at LET of 60	4
PCA80C522	Processor	9707	Phillips	H: (BNL01AUG) JH/KL	SEL	SEL $LET_{th} > 3$; $\sigma_{sat} > 3x10^{-3}$	3

* Category rating applies only for SEL not for other SEE concerns. All parts tested to a minimum fluence of 1.0×10^7 particles/cm^2

TABLE IX: SUMMARY OF PROTON DAMAGE TEST RESULTS **

Part Number	Function	LDC	Manufacturer	Particle: (Facility,Date)P.I.	Testing Performed	Summary of Results
Misc.:						
BAE CCD486	ACS 4kx4k WFC CCD Detector	3188	British Aerospace	P: (UCD01MAR) MJ/RR/PM	DD	CTE degraded to <0.99999 at $2.5x10^9$ p/cm^2 at 63 MeV; CTI (I-CTE) increases by factor of ~2 from 2.5 to $5x10^9$ p/cm^2
TIL25	GaAs LED	N/A	Texas Instruments	P: (UCD01MAY) SK/JH/RR	DD	Significant degradation in LED power at total fluence of $2.56x10^{10}$p/cm^2 at 63 MeV
TIL601	Opto Transistor	N/A	Texas Instruments	P: (UCD01MAY) SK/JH/RR	DD	Significant degradation in collector current at total fluence of $6.4x10^{10}$p/cm^2 at 63 MeV
4N49	Optocoupler	9803 and 9818	Micropac	P: (UCD01MAY) SK/RR	DD	V_{CE} values varied widely with application voltage. Slight to significant degradation in V_{CE} seen at $1x10^{11}$p/cm^2
AD8151	Crossbar Switch	LA 1148.4	Analog Devices	P: (UCD02JAN) SB/PM/RR	P: TID (also see SEE table)	Shows no changes in supply current up to a TID of 14 krad(Si) Degradation in performance at ~70 krad(Si); current increased with dose up to 168 krad(Si) Note: Functionally tested only - Not full TID parametric evaluation

** Radiation damage effects are not categorized.

TABLE X: SUMMARY OF TID TEST RESULTS

Part Number	Function	LDC	Manuf.	Particle: (Facility,Date)P.I.	Testing Performed	Summary of Results	Cat.
ADCs:							
AD7714	24 bit ADC	0041	Analog Devices	(NAVSEA02FEB) CP/JB	TID	Non-functional between 10 krad(Si) and 20 krad(Si) Degradation between 7.5 krad(Si) and 20 krad(Si) No degradation in integral nonlinearity up to 10 krad(Si)	2
LTC1272	12 bit ADC, 250 kHz	0018	Linear Technologies	(NAVSEA01DEC) CP/JB	TID	Parametric failures were observed at 5 krad(Si) on all devices	2
AD6640	12 bit ADC, 65 MHz	9951	Analog Devices	(NAVSEA01NOV) JH/JB	TID	No significant degradation to 100 krads(Si)	1
Power MOSFETs:							
FDN361AN	30V N channel MOSFET	0133	Fairchild	(NAVSEA01DEC) JT/CP	TID	Within specification up to 20 krad(V_{th})	2
NDS352A	30V P channel MOSFET	0053	Fairchild	(NAVSEA01DEC) JT/CP	TID	All parameters within specification at 50 krad(Si)	2
IRLML2803	30V N channel MOSFET	0103	International Rectifier	(NAVSEA01DEC) JT/CP	TID	Within specification up to 35 krad(Si) (V_{th})	2
IRLML5103A	30V P channel MOSFET	0034	International Rectifier	(NAVSEA01DEC) JT/CP	TID	Within specification up to 35 krad(Si) (Rds_{ON})	2
2N5114	30V P channel JFET	9518	New England	(NAVSEA02JAN) JT/CP	TID	IDSS and IGSS exceeded their specification limit at 50 krad(Si)	2
Misc:							
Pentium III 550, 650, 700, 800, 850, 933 MHz and 1 GHz	Processor	S-spec: SL3V5 SL452 SL454 SL457 SL47M SL47Q SL4KK	Intel	(GSFC02JAN) JH	TID	Biased (operating): Functional failure levels are 500-600 krads(Si); Unbiased: Functional failure levels > 3 Mrads(Si)	1

IV. SEE Test Results and Discussion

This section contains GSFC test results including test method, SEE or degradation conditions/parameters, and graphs of data.

A. Op Amps & Analog Comparators:

1) LM124

National Semiconductor LM124 Op Amp was tested for SET at BNL and NRL (laser facility). Four different applications were investigated for the LM124: voltage comparator, non-inverting gain (x101), non-inverting gain (x11), and voltage follower using different power supply and input bias conditions.

The output of the DUT was monitored with a digital oscilloscope. As soon as the DUT output exceeded a preset trigger level (generally 500 mV), an SET is counted and the complete SET transient data was stored on a computer for future analysis.

Heavy ion testing was performed at TAMU. The LM124 results showed a large variety of transient waveforms and a significant impact of the power supply voltage.

The LM124 exhibited a very low sensitivity when used as a voltage comparator and a higher SET sensitivity when used as a non-inverting gain amplifier or a voltage follower. Figure 1 shows the worst case SET cross section curve for the non-inverting-gain-of-11 application. The LET_{th} is lower than 2.86 MeVcm^2/mg and the maximum cross section is about 3x10^{-5} cm^2/amplifier.

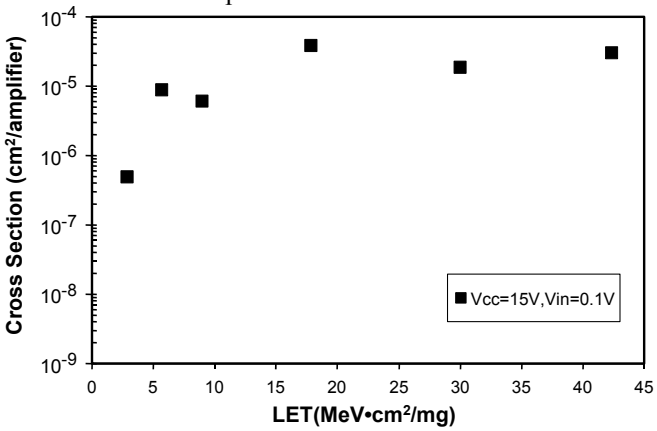

Figure 1: LM124 SET cross section curve, non-inverting gain of 11.

These worst case results were obtained with a +/-15V power supply voltage for both input voltages investigated. The worst case cross sections for the non inverting gain of 101 and the voltage follower applications were similar for the +/-15V power supply voltage, but we see an effect of the input voltage near the LET_{th}. Near the threshold, the lower input voltages give the higher SET sensitivities.

When the power supply voltage was +5V/0V, the SET sensitivity was significantly lower for high input voltages. In these conditions, no event was observed at an LET of 9 MeVcm^2/mg and only a few events have been observed at an LET of 30 MeV•cm^2/mg.

Three different types of transients were seen. First, large bipolar transients were predominant, especially at low LET. The transient's negative going component characteristics depend strongly on the application (the higher the gain the lower the amplitude and the shorter the duration). The overall transient characteristics vary with the LET. Second, long duration positive going transients only appear at high LET and may account for up to 35% of the total number of transients. Finally, small positive going transients that are negligible at low LET and could represent up to 25% of the total number of transients at high LET.

An example of a large bipolar transient is shown in Figure 2. The transient's positive going component goes up to the +Vcc rail, and it has a 1.5 μs full width half maximum (FWHM). The worst case amplitude of long duration transients was 2V and their maximum FWHM was longer than 10 μs. The worst case amplitude of a small transient is 2V. The worst case FWMH is 600 ns. For more details see "Single Event Transients in LM124 operational amplifier Laser test report". [11] and "Development of a Test Methodology for Single Event Transients (SET) in Linear Devices" [3]

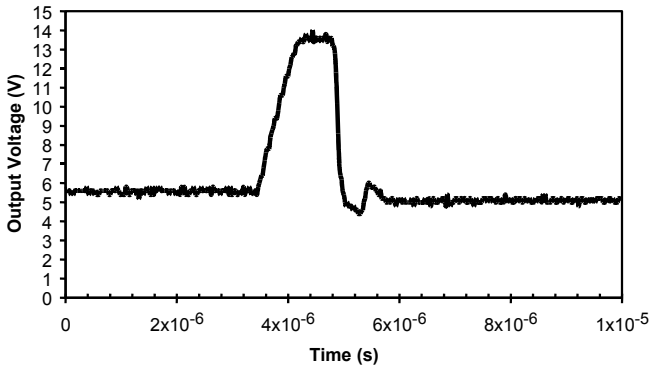

Figure 2. LM124, Non-inverting gain x101 application, typical large bipolar transient, LET = 2.86 MeV•cm^2/mg, Vcc = +/- 15V, V+ = 0.05V.

2) LM119

SET testing was performed on the National Semiconductor LM119 voltage comparator at BNL. The dependence of the SET cross section on supply voltage, differential input voltage and output load were measured. The LM119 was tested under the following conditions:

- V_{DD} = 5V, 10V, and 15V
- Δ V = +4.5V, +2.5V, +0.12V, -0.2, and –4.5V
- Load resistance (R) = 1.7 KΩ and 0.17 KΩ
- Angles = 0^o and 60^o
- LET = 11.44 MeV•cm^2/mg, 24.21MeV•cm^2/mg and 59.87 MeV•cm^2/mg

The cross section for positive differential input voltage was an order of magnitude smaller than for negative differential input voltage, confirming the results seen during pulsed laser testing. Figure 3 shows the cross section as a function of LET for both positive and negative values of ΔV. Figure 3 also shows that the cross section increases at higher positive values for ΔV but does not do so for negative values of ΔV. Figure 4 shows that the cross section increases with increasing supply voltage. In addition, there

was no dependence of the cross section on the output load, which was varied by a factor of 10. [4] [5]

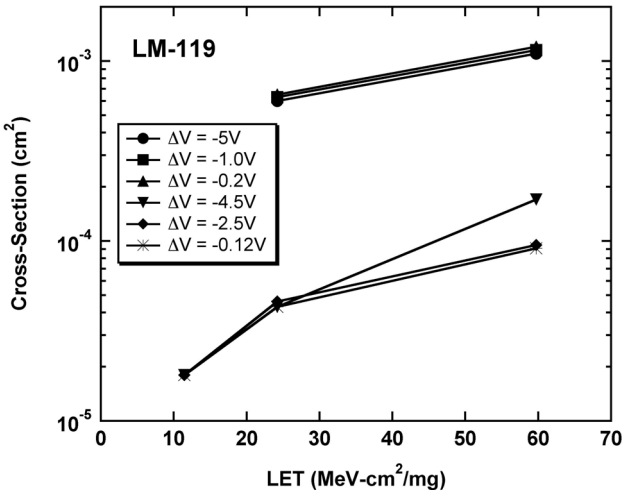

Figure 3. SET cross section as a function of ion LET for the LM119 voltage comparator for positive and negative differential input voltages. The cross section is an order of magnitude greater for negative differential input voltage than for positive differential input voltages.
Also, at an effective LET of 60 MeV.cm^2/mg, the cross section for $\Delta V = 4.5$ V is greater than at 2.5 V.

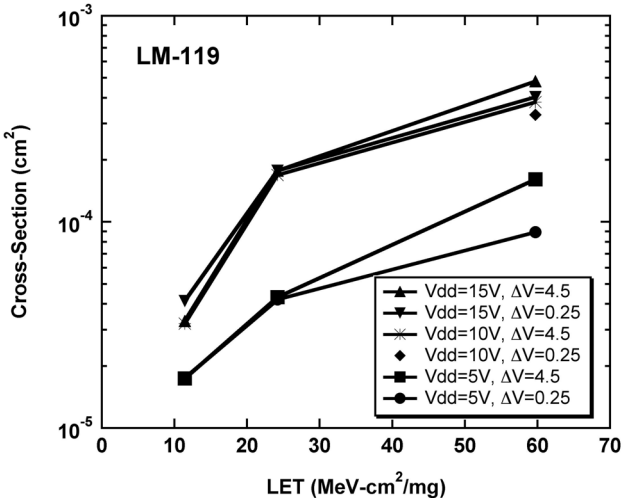

Figure 4. SET cross section as a function of ion LET for the LM119 voltage comparator for different combinations of supply voltage (V_{DD}) and differential input voltage (ΔV). The general trend is that the cross section is larger for larger supply voltages.

B. Programmable Devices:

All 22V10 devices were tested as follows: The power supply was set at +5V with nominal current. The DUTs were driven at 1MHz. The devices were configured/programmed identically. Outputs 1-4 count from 1 to 15. Output 5 is a Carry Out, which senses the end of the count to 15, drives the Output Low, then back to High. Output 6 is a Flip-Flop, toggling from 0 to 1 with each clock pulse. Outputs 1-6 are compared to a reference DUT (an Atmel device with the identical program loaded) to look for SET. Output 7 is High, Output 8 is Low; both are compared with an exclusive NOR to look for SEL. The test program can distinguish mismatch SET, SEFI, SEL, High/Low SET, and Timing Error SET.

1) PALCE22V10

The Cypress programmable array logic PALCE22V10 was tested for SEFI, SEL and SET at BNL. The DUTs exhibited SEFI and one non-destructive SEL at an LET of 7.9 MeV•cm^2/mg. Typically, the SEFI occurred simultaneously with ~110-130 errors from Outputs 1-6 while the counter monitoring the High and Low rail of the device counted every clock cycle as one of the rails had failed. Each time the device recovered after a power cycle. Nominal current was 76mA; during one run, the DUT latched and the power supply current went to 110mA; the current and functionality recovered after a power cycle. A summary of all effects is given in Table 11. [12]

2) ATF22V10B

The Atmel Electronically Erasable (EE) programmable logic device ATF22V10B was tested for SEL and SET at BNL. The DUTs showed no SEL up to an LET of 84.4 MeV•cm^2/mg. There were a few SET mismatch errors, with the cross section tending to increase slightly with increasing LET. The mismatch LET_{th} was < 13.2 MeV•cm^2/mg. Additionally, the software could detect timing errors when they occur and separately from other mismatch errors in Outputs 1-6. These timing errors were detected in several runs, the timing error LET_{th} was < 23 MeV•cm^2/mg. The High/Low comparator also saw an increasing number of SETs with increasing LET, with a comparator $LET_{th} < 11.44$ MeV•cm^2/mg. A summary of all effects is given below in Table 11. [12]

3) GAL22V10/883

The Lattice E^{2}CMOS generic array logic GAL22V10/883 was tested for SEL and SET at BNL. The DUTs showed a non-destructive SEL with an $LET_{th} < 26.6$ MeV•cm^2/mg. Typical I_{CC} was ~20mA and the SEL took the current to 99-110mA. The devices recovered after a power cycle. These events also led to the High/Low rail counter monitor to count all clock cycles as in the case of the Cypress parts. There were very few SET mismatch errors, typically one or two per run. The mismatch errors LET_{th} was < 22.9 MeV•cm^2/mg. Additionally, timing errors were detected in four runs with the same onset as that of the mismatch errors. A summary of all effects is given in Table 11. [12]

TABLE 11: SUMMARY OF SEE FOR 22V10 DEVICES*

Manu-facturer	Mismatch SET	SEFI	SEL	High/Low SETs	Timing Error SETs
Cypress PALCE22V10	Occurred with SEFI	$LET_{th} < 7.9$	One observed at an LET of 7.9	Continuous errors with SEFIs or SEL	Some occurred with SEFIs
Atmel ATF22V10B	$LET_{th} < 13.2$	None detected	$LET_{th} > 84.4$	$LET_{th} < 11.4$	$LET_{th} < 23$
Lattice GAL22V10/883	$LET_{th} < 22.9$	None detected	$22.9 < LET_{th} < 26.6$	$LET_{th} < 11.4$ but there are continuous errors with SELs	$LET_{th} < 22.9$

* All numbers given are in MeV•cm^2/mg.

4) AN10E40

Heavy ion testing was performed at BNL on the AN10E40 Field Programmable Analog Array (FPAA) manufactured by Anadigm. The test setup was comprised of an Anadigm evaluation board that housed the DUT. Using the evaluation board, a configuration of the gain stage of 5 was used on the DUT. A function generator provided a 1kHz signal, riding on a 2.5V rail, to the input and the output with a gain of 5 was captured using a digitizing oscilloscope. The scope's built in counter was used to count the number of triggers (SETs). A power supply provided input voltage to the DUTs.

DUTs experienced SETs and loss-of-configuration errors at an LET of 11.44 MeV•cm^2/mg. One DUT experienced transient errors with the beam off after approximately 10 krads(Si) total dose. Another DUT also experienced SEL at an LET of 19.9 MeV•cm^2/mg. For this device, 18 < SEL LET_{th} < 19.9. The SELs caused the current to the test board to increase from 50 mA to >90 mA. The device recovered after power cycling. [13]

C. Power Devices:

1) MDI3051RES05ZF, MDI3051RED12ZF, and MDI3051RED15ZF

The Modular Devices, Inc. MDI3051RES05ZF, MDI3051RED12ZF and MDI3051RED15ZF DC/DC Converters were monitored for heavy ion induced transient interruptions in the output signal and for destructive events during testing at TAMU. These tests were performed at a flux of $4x10^4$ to $6x10^4$ particles/cm^2/s. All DC/DC converters tested were de-lidded and the active device area divided into three circular regions. Region number 1 included the power MOSFET, Region #2 contained the linear devices at the device output and Region #3 was a linear device near the MOSFET.

The test hardware for this testing included a digitizing oscilloscope, programmable power supplies and an electronic load. The programmable power supplies were used as input to the DC/DC converter, allowing remote control of the input voltage. The output from the devices was swept across the high impedance input of the digital scope and into an electronic load that maintained constant device loading via a constant current mode on the output of the device. Any transients that appeared on the output pins of the devices were captured and saved to a file. A destructive event was said to have occurred whenever the device output shifted to to a value outside the specifications and could not be restored even by cycling power to the device.

During testing, device temperature was monitored and remained between 20 and 25°C. A single sample of each device type was irradiated with ions having LETs ranging from about 20 to 60 MeV•cm^2/mg while operating under different input-voltage and load conditions. No single-event transients were seen in any of the irradiations, but destructive failures were observed for each device for some conditions of voltage and load. These failures resulted in the output voltage dropping to 0 and device functionality being lost. The MDI3051RES05ZF failed under irradiation with Kr ions with LET=37 MeV•cm^2/mg while operating at 126 V and 75% loading. However, because this was the first test run with loading greater than 50%, vulnerability at lower LET cannot be ruled out. No failures were seen for:

- 75% loading at 120 V at an LET of 28.4
- 75% loading at 126 V at an LET of 28.4
- 50% loading at 120 V at an LET of 37
- 25% loading at 120 V at an LET of 37

The MDI3051RED12ZF was seen to fail under irradiation with Xe ions with LET=60 MeV•cm^2/mg while running at 120 V and 50% loading. Prior to that failure, the device successfully ran through approximately 10^7 ions/cm^2 at four other test conditions, including:

- 75% loading at 120 V at an LET of 28.4
- 75% loading at 126 V at an LET of 28.4
- 50% loading at 120 V at an LET of 37
- 25% loading at 120 V at an LET of 60

The MDI3051RED15ZF was seen to fail under irradiation with Xe ions with an LET of 60 MeV•cm^2/mg while operating under the 120 V, 75% loading condition. Prior to that failure, the device successfully ran through approximately 10^7 ions/cm^2 at the other test conditions, including:

75% loading at 120 V at an LET of 37
75% loading at 126 V at an LET of 37
25% loading at 120 V at an LET of 60
[14] [15] [16]

2) LM2651

The monolithic switching regulator LM2651 from National Semiconductor was tested at BNL using ions with effective LETs ranging from 11.4 MeV•cm^2/mg to 37.5 MeV•cm^2/mg. Three different load conditions were tested (no load, 40% and 60% of a maximum load of 400 mA). The transient LET_{th} was about 5 MeV•cm^2/mg. The SET cross section measured at the maximum LET of 37.5 MeV•cm^2/mg was ~$1.5x10^{-4}$ cm^2/device. The three parts experienced destructive failures. The highest load appeared to be the worst case configuration for destructive failures. No failure was observed up to a LET of 26 MeV•cm^2/mg and a fluence of $1x10^7$ ions/cm^2 for all load conditions. The first failure occurred at a LET of 37.4 MeV•cm^2/mg for the maximum load condition. The failure cross section at the maximum tested LET is about $2.5x10^{-6}$ cm^2/device. On two parts (SN1 and SN2) the output voltage was at 0 V after the failure. On SN3, the output voltage was equal to +Vin (10V) after the failure. On SN1 and SN3, the failure occurred at the bonding pad of one of the device output power MOSFETs as shown in Figure 5. As shown in the picture, the bonding pad was vaporized. No apparent failure was observed on the MOSFET. [17]

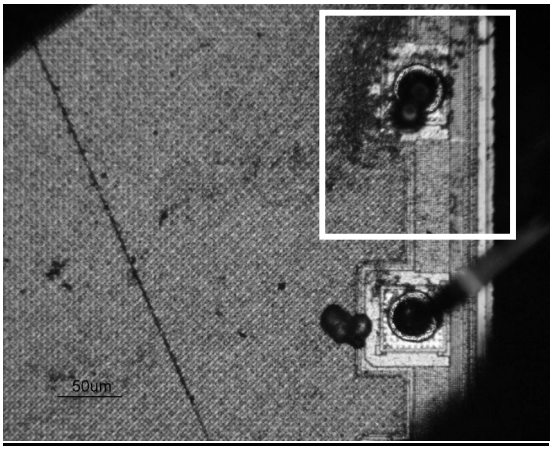

Figure 5: Picture of the vaporized bonding at the output MOSFET of the LM2651.

3) MSK5042

The MS Kennedy MSK5042 hybrid switching regulator was tested for SET and SEB sensitivity at BNL. This part uses four different SEE sensitive device types: one pulse width modulator (PWM) controller MAX797 from MAXIM, two 55V N-channel power MOSFET IRLC034N from International Rectifier, one voltage reference REF43 from Analog Devices, and one operational amplifier AD822 from Analog Devices. The part was biased with the 30V maximum input voltage. The output voltage was adjusted to 2.5 V. This part was tested for SET and SEL at BNL using ions with an effective LET ranging from 11.4 to 84 MeV•cm^2/mg. The PWM controller was irradiated alone, and the four other sensitive devices have been irradiated together. Figure 6 shows the two different irradiated areas. A low transient sensitivity was observed for both areas. When the MOSFET and linear area were irradiated, two failures were observed, one at an LET of 59 MeV•cm^2/mg and the other at an LET of 37 MeV•cm^2/mg. These failures were attributed to Single Event Burnout on the power MOSFETs. Figure 7 shows the failure on one power MOSFET. [18]

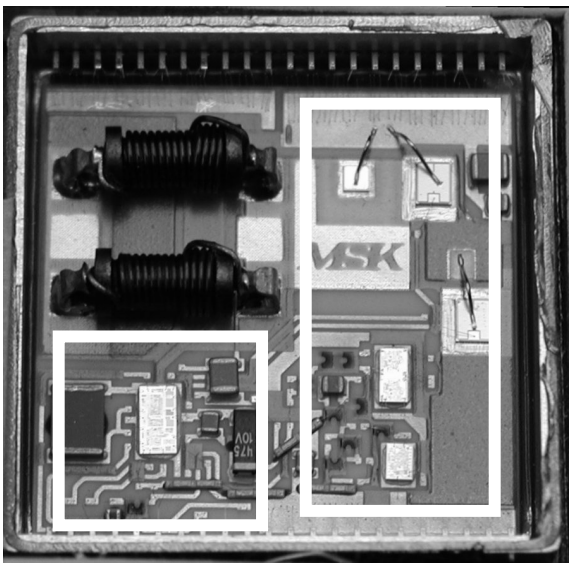

Figure 6: Irradiated area, first area on the left includes the MAX797, second area includes the power MOSFETs, the voltage reference, and the operational amplifier.

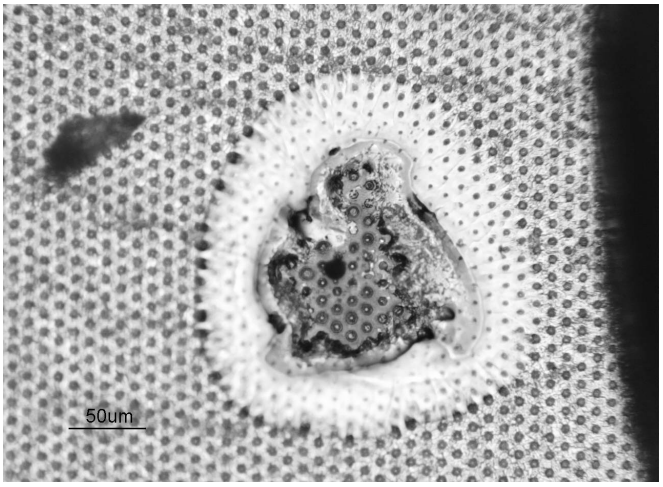

Figure 7: Burnout on a power MOSFET.

4) LP3470

The LP3470 power on reset circuit from National Semiconductor was tested at BNL using ions with an effective LET ranging from 1.4 MeV•cm^2/mg to 27 MeV•cm^2/mg. During testing the device reset output was monitored by an oscilloscope. As soon as the output deviates by more than 2V from the nominal value, an error is counted. The device is extremely sensitive, with 1 active reset at the lowest LET for a fluence of 1x10^7 ions/cm^2. The cross section then increases very rapidly to about 8x10^{-5} cm^2/device at a LET of 2.5 MeV•cm^2/mg. Above a LET of 11 MeV•cm^2/mg, the reset output stays continuously activated and cross sections were able to be measured at normal flux rates. [19]

D. ADCs and DACs:

1) AD7714

The Analog Devices AD7714 500 µA, 100 kHz, 24 bit signal conditioning ADC was tested for SEE at BNL. The part features three differential analog inputs (which can also be configured as five pseudo-differential analog inputs) as well as a differential reference input. The AD7714 thus performs all signal conditioning and conversion for a system consisting of up to 5 channels. The digital data is available via a serial interface. This serial interface is also used to configure the ADC gain settings, signal polarity and channel selection.

The AD7714 evaluation board was used for the SEE testing. A program was written that allowed part configuration, acquisition of the serial data during the conversion, and monitoring of the conversion errors. Because the part includes many configuration registers, upsets in these registers could cause SEFIs. As soon as 10 successive converted words were in error, we assumed a SEFI and the part was reconfigured. The device supply current was also monitored during the irradiation. As soon as this current reached a limit of 50 mA, the power supply was shutdown. A static 1V input voltage was applied during the irradiation (for a full scale signal of 2.5V). With this setup, we were able to test the 16 most significant bits (MSB) out of the 24 bits.

The Figure 8 shows the SEU and SEL cross section curves. Due to the high SEL sensitivity, it was not possible to perform a SEU characterization for LET above 16 MeV•cm^2/mg. The SEU LET$_{th}$ was about 3 MeV•cm^2/mg and the device SEU cross section is about 6x10^{-5} cm^2 at an LET of 16 MeV•cm^2/mg. Some SEFI were observed during the experiments. Most of the errors were multiple errors within a corrected word, and the MSB were as sensitive as the Least Significant Bit (LSB) tested. The SEL LET$_{th}$ was about 16 MeV•cm^2/mg (no SEL event was observed at a LET of 15 MeV•cm^2/mg up to a fluence of 1x10^7 ions/cm^2), the device SEL cross section was about 3x10^{-4} cm^2 at an LET of 50 MeV•cm^2/mg. The peak latchup current was between 40 and 60 mA (the nominal power supply current is about 0.8 mA). Figure 9 shows a typical latchup current waveform.

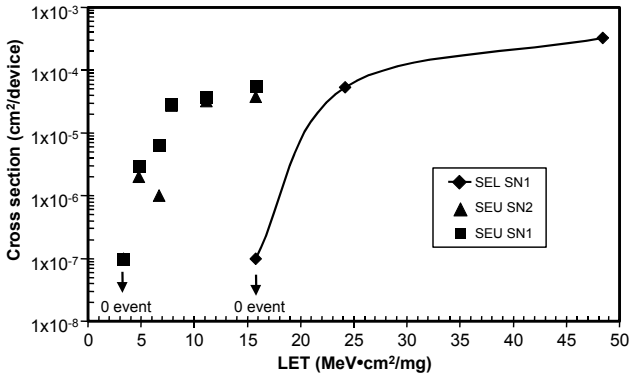

Figure 8: AD7714 SEU and SEL cross section.

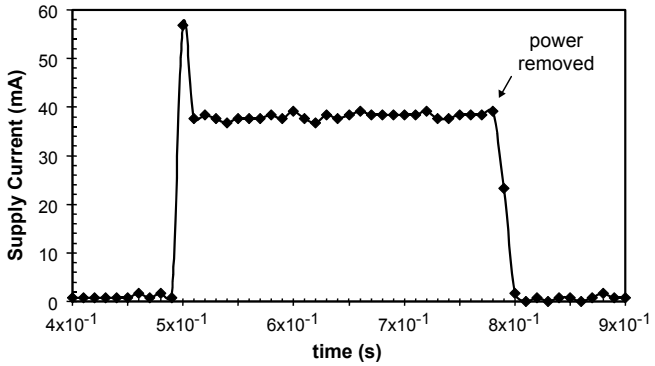

Figure 9: Typical Latchup current waveform for the AD7714.

2) AD7821

The 8 bit ADC AD7821 from Analog Devices was tested for SEU and SEL at TAMU using ions covering an LET range from 1.8 to 80 MeV•cm^2/mg. The test used the golden chip method [20] in which the same input signal was sent to the DUT and a reference device that was not irradiated. The outputs of the two devices were compared and the errors were counted and recorded. Static input signals were applied and only the 7 MSB were tested. No SEL events were observed up to the maximum tested LET of 80 MeV•cm^2/mg and a fluence of 6x10^6 ions/cm^2. The SEU LET$_{th}$ (~4) of the 4 MSBs and the 3 LSBs was the same, but the maximum SEU cross section of the MSBs was significantly higher than that of the LSBs (ratio >2). The total SEU cross section curve for the 7 tested bits is shown in Figure 10. [21]

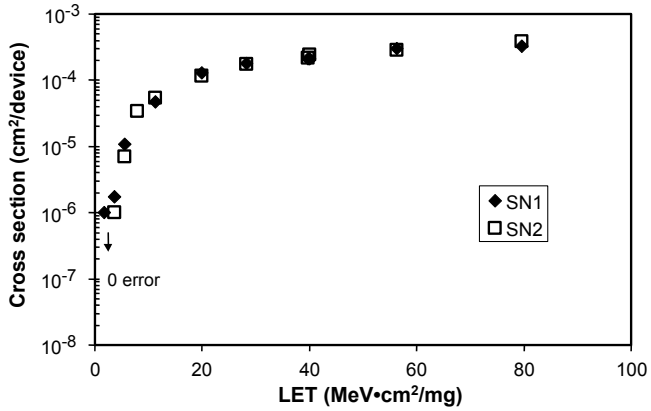

Fig 10: AD7821 SEU cross section curve

3) AD9223

The 12 bit ADC AD9223 from Analog Devices was tested for SEU and SEL at TAMU using ions covering a LET range from 1.8 to 40 MeV•cm^2/mg. The golden chip method was used for testing [20]. The outputs of the two devices were compared and the errors were counted and recorded. Static input signals were applied and only the 7 MSB have been tested.

The device exhibited SEL sensitivity at an LET of 20 MeV•cm^2/mg. The SEL cross section at the maximum tested LET of 40 MeV•cm^2/mg was about 1x10^{-4} cm^2/device. The SEL cross section curve is shown in Figure 11.

The SEU sensitivity of the 4 MSBs was very low. The LET$_{th}$ was less than 11.2 MeV•cm^2/mg where only a few SEU were observed. The LET$_{th}$ for the 3 medium bits (bits 5,6,7) was about 1.8 MeV•cm^2/mg and the SEU sensitivity of these bits (bits 5,6,7) dominated the SEU response of the 7 tested bits. We would expect a higher sensitivity in the 5 LSBs that were not tested. The SEU cross section curve is shown in Figure 11. [21]

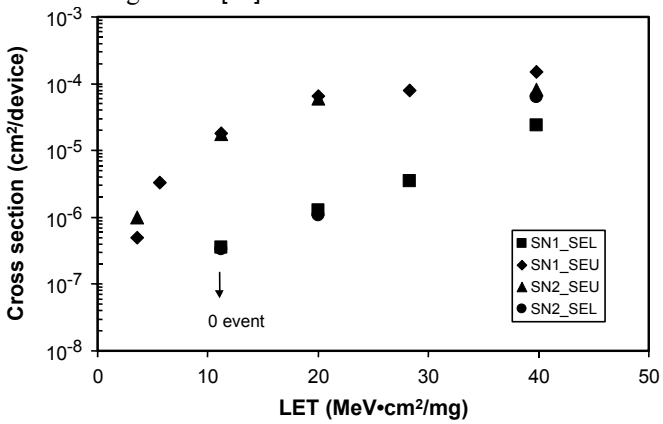

Figure 11: AD9223 SEU and SEL cross section curve.

4) LTC1272

The 12 bit ADC LTC1272 from Linear Technology was tested for SEU and SEL at TAMU using ions covering a LET range from 1.8 to 20 MeV•cm^2/mg. The same input signal was sent to the DUT and a reference device that was not irradiated. The outputs of the two devices are compared and the errors were counted and recorded. Static input signals were applied and only the 7 MSB were tested.

This device was very sensitive to SEL; the SEL LET_{th} was less than 5.6 MeV•cm^2/mg and the cross section at the maximum tested LET of 20 MeV•cm^2/mg was $1x10^{-4}$ cm^2/device. The SEL cross section curve is shown in Figure 12.

The SEU sensitivity of the 3 medium bits tested dominated the SEU response of the 7 tested bits. The LET_{th} of the 4 MSBs was less than 4 MeV•cm^2/mg where the number of errors was low. The LET_{th} of the 3 medium bits (bits 5,6,7) was less than 1.8 MeV•cm^2/mg and the number of errors was very high. We could expect a higher sensitivity of the 5 LSBs that were not tested. The SEU cross section curve is shown in Figure 13. [21]

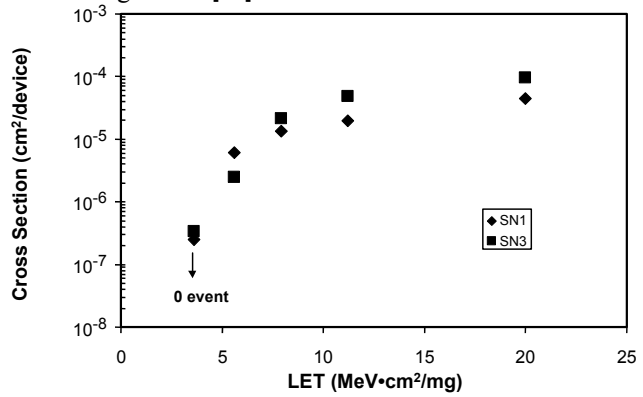

Figure 12: LTC1272 SEL cross section curve.

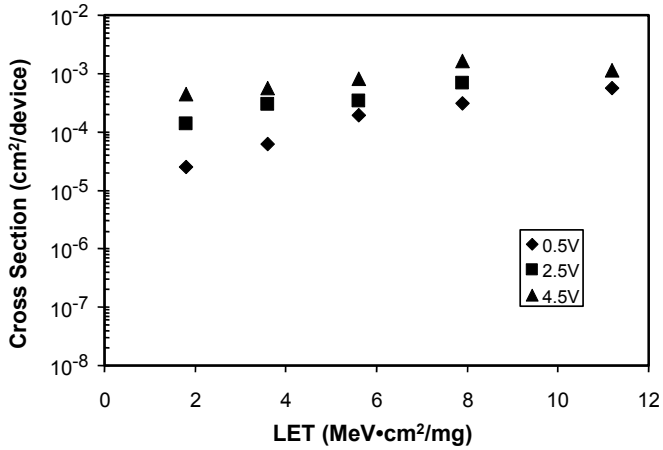

Figure 13: LTC1272 SEU cross section curve.

5) LTC1657

The 16 bit Digital to Analog Converter LTC1657 from Linear Technology was tested for SEU and SEL at BNL using ions covering a LET range from 3.4 to 37 MeV•cm^2/mg (Bromine at 0 degree). The setup allowed the distinction between the transient errors (glitch at the device output) and the permanent errors (Single Event Upset in the device registers). A static digital input was applied during the irradiation (about mid scale, DUT input=2V). With this setup we were able to test the 11 MSBs out of the 16 bits device resolution.

The device was not sensitive to SEL up to a LET of about 14 MeV•cm^2/mg. The SEL cross section was about $6.3x10^{-5}$ cm^2/device at an LET of 37 MeV•cm^2/mg. The SEL cross section curve is shown in Figure 14. During a SEL the part was non-functional, but after a power cycle the device recovered its functionality. The latchup current was about 54 mA (nominal current was 0.7 mA).

Figure 14 shows the cross section curves of the SEU sensitivity and the total device error sensitivity. Most of the errors are SEU that occur in the device registers, but at high LET a significant number of transient errors are observed. The SEU LET_{th} is about 4 MeV•cm^2/mg and the cross section is $3.8x10^{-4}$ cm^2/device at an LET of 37 MeV•cm^2/mg. The cross section of the total number of errors is $1.2x10^{-3}$ cm^2/device at an LET of 37 MeV•cm^2/mg. [22]

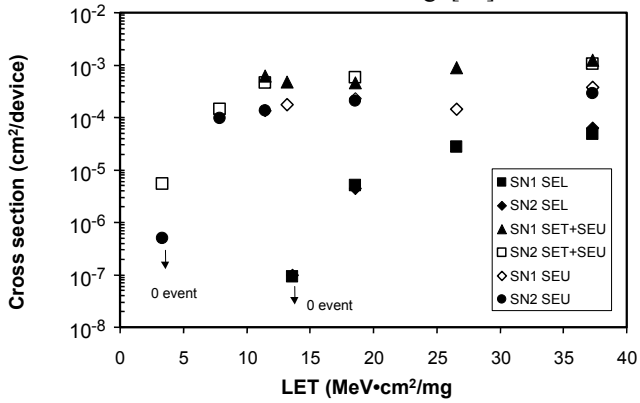

Figure 14: LTC1657 SEU and SEL cross section curve.

6) ADC1175

The 8 bit ADC ADC1175 from National Semiconductor was tested for SEU at BNL using ions covering an LET range from 3 to 49 MeV•cm^2/mg and SEL tested at TAMU using ions covering an LET range from 11 to 118 MeV•cm^2/mg.

The National semiconductor ADC1175 evaluation board was used for the SEE testing. This board operates the AD1175 from a single +5V supply at a 20 MHz clock. Before each irradiation, the device digital output was stored in an 8 bit register. Then, during the irradiation, the DUT output was compared to the register content. In case of a difference, an error was counted. Input voltage during the experiment was 4.5V.

The device was not sensitive to SEL up to an LET of ~23 MeV•cm^2/mg. The SEL cross section is about $4.6x10^{-6}$ cm^2/device at an LET of 118 MeV•cm^2/mg.

The device has a significant SEU/SET sensitivity with a LET_{th} lower than 3 MeV•cm^2/mg and a device SEU/SET cross section of $4.5x10^{-4}$ cm^2/device at an LET of 49 MeV•cm^2/mg. The SEU/SET cross section curve is shown in Figure 15.

No SEFI was observed during any of the experiments. [23]

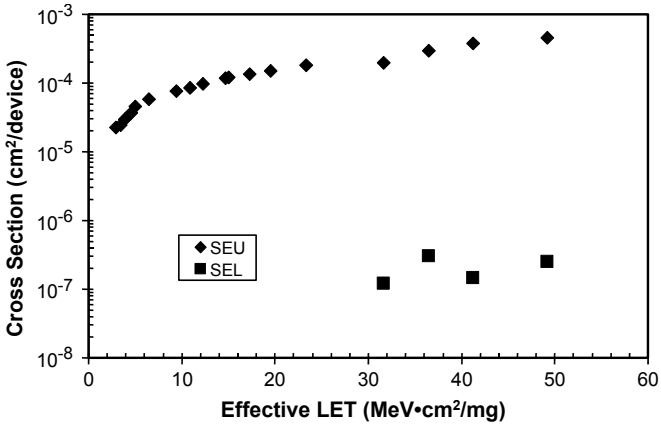

Figure 15: ADC1175, SEU and SEL cross section curve (TAMU).

E. Communication Devices:

1) 1394 FireWire chipsets including TSB12LV26PZT, and TSB41AB3PFP, from TI and the CS4210VJG, and CS4103VHG from National Semiconductor

Radiation tests were performed on IEEE 1394 Open Host Controller Interface (OHCI) Chipsets from two manufacturers, Texas Instruments (TI) and National Semiconductor (NSC), to evaluate Single Event Effects. Four parts were tested in two different modes at three different facilities, BNL, TRIUMF and TAMU Facilities. Many types of SEFIs were observed which required intervention to correct - from software bus resets to the more severe cable reset and power cycling with both protons and at low LET heavy ions. Serious mitigation concerns must be addressed in order to use these parts. The NSC parts exhibited destructive latchup when exposed to ions with a LET of 27 MeV•cm^2/mg. See [6], [24], and [25].

2) Myrinet Devices

Myricom Myrinet crossbar switches and a network interface card (NIC) were exposed to the 63 MeV proton beam at UCD to perform a proton SEE evaluation. Proton-induced SEUs and SEFIs were observed at the system level for both the crossbar switches and for five devices exposed on the NIC. SEU cross section for the crossbar switch was approximately $5x10^{-13}$ cm^2, on average and ranged from $5x10^{-12}$ to $8x10^{-11}$ cm^2 for the NIC, depending on which device was exposed. The SEFI cross section for the crossbar switch was approximately $5x10^{-13}$ cm^2 and ranged from $3x10^{-12}$ to $4x10^{-10}$ cm^2 for the NIC, depending on which device was exposed. The complete details on the testing and results can be found in this year's Data Workshop paper entitled "Proton Single Event Effects (SEE) Testing of the Myrinet Crossbar Switch and Network Interface Card", [7], also a detailed test report is available [26].

3) AD8151

SEE testing of the Analog Devices AD8151 crossbar switch was carried out at the TAMU and CNL facilities. LETs ranged from 2.86 to 60 MeV•cm^2/mg. A Bit Error Rate Tester (BERT) was used to provide a serial stream of data ("1s" and "0s") to the input of the AD8151. Two configurations were tested to evaluate the BER dependence on the number of switches through which the signal passed. In the first configuration a single input was connected through the switch matrix to a single output. In the second configuration, the signal from the BERT passed through the switch five times.

The AD8151 Cross Point Switch exhibited two types of single-event effects. The first consisted of a temporary loss of transmission caused by heavy ion strikes to the switches themselves, resulting in bursts of errors whose length depended on ion LET. The second consisted of a complete cessation of transmission caused by heavy ion strikes to the registers containing the data specifying the switch configuration. Only by rewriting the data to the registers could data transmission be restarted. The part was latchup-free to a LET of 60 MeV•cm^2/mg to a fluence of $6.55x10^5$ p/cm^2 and showed no changes in supply current up to a TID of 14 krad(Si) from 63 MeV protons. Both the heavy ion and proton cross sections depended on operating conditions. [27] [28] [29]

4) LSP2916

The Agere Systems LSP2916 16-channel, high voltage driver for microelectromechanical systems (MEMS) was tested for SEE at BNL. Two device types were tested, the "A" version with –33V/V gain and the "B" version with -66V/V gain. The devices were tested at BNL. The devices showed no evidence of SETs on the output during testing.

The device exhibited a destructive SEL at an LET of 26.6 MeV•cm^2/mg. No event was observed at an LET of 13.2 MeV•cm^2/mg. Thus, the SEL LET_{th} was between 26.6 MeV•cm^2/mg and 13.2 MeV•cm^2/mg. The SEL rendered the entire device non-functional due to the partial vaporization of the V_{LP} (5V power supply) bond wire (A type, -33V/V gain devices) or the complete vaporization of the V_{LP}, V_{HN} (high voltage negative supply) and Ground bond wires. See Figures 16 and 17 for views of DUT 2 (B type, -66V/V gain devices). When the SEL occurred, in all cases, a spark was visible in the test vacuum chamber on a closed circuit TV monitor. For example, while being irradiated at an LET=26.6 MeV•cm^2/mg, an "A" type device abruptly ceased functioning following an SEL (indicated by a flash on the monitor) and then spontaneously (without power cycling) began to function again after a few seconds. This may indicate latent damage. [30] On the subsequent run the part failed due to SEL and did not recover. [31]

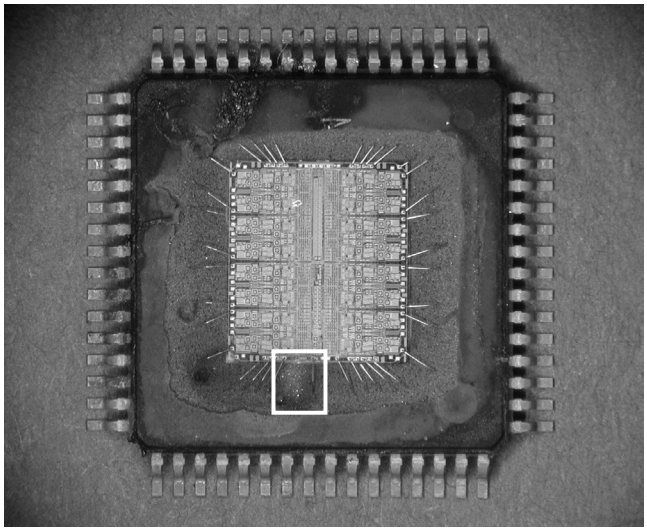

Figure 16. View of complete LSP2916 device with vaporized bond wires . See detail of boxed region in Figure 17.

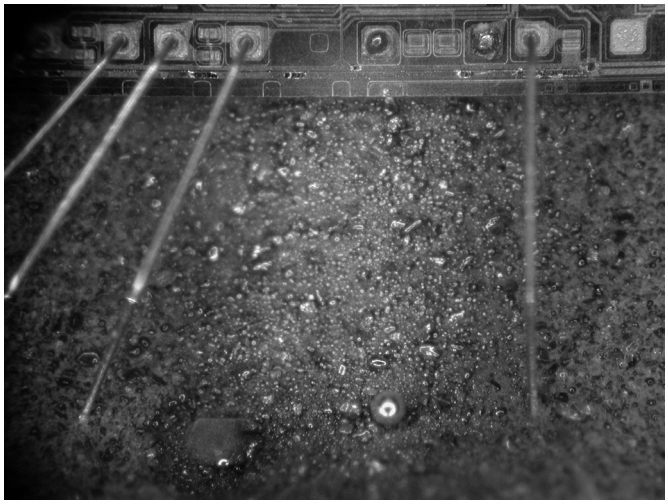

Figure 17. LSP2916 DUT 2 detail view of V_{LP} and ground wires. Note the deposition of the gold bond wires on the exposed die (in the center of the picture) as well as damage to the metal trace.

5) APS Photobit

The Photobit active pixel sensor (APS) was tested for SET at TAMU. Measurements were made using Ar-40 at 15.0 MeV/amu, Kr-84 at 15.3 MeV/amu, and Xe-131 at 15.2 MeV/amu. The heavy ion single event transient response of Photobit APS subarrays was very dependent on the specific pixel design. No latchup was observed up to an LET of 106 MeV/mg/cm2 (Xe at 60^{o}) for a fluence >2x10^{7}/cm^{2} [8].

6) Test Sample 5HP SiGe Prescaler

This IBM SiGe Heterojunction Bipolar Transistor (HBT) BiCMOS technologies, 5HP series was tested at UCD/CNL (Protons) and TAMU (Heavy Ions). Bit upsets were seen with 63MeV protons. For more information see "Single Event Upset Test Results on an IBM Prescaler Fabricated in IBM's 5HP Germanium Doped Silicon Process," [9].

7) PE9301

The Peregrine divide-by-2 prescaler fabricated in Ultra Thin Silicon (UTSi) 0.5um Silicon On Sapphire (SOS) process was tested at UCD/CNL (Protons) and TAMU (Heavy Ions). Bit upsets were see for 63MeV protons. For more information see "Effects of Proton Beam Angle-of-Incidence on Single-Event Upset Cross-Section Measurements," [10].

8) MTX8501 and MRX8501

The Emcore MTX8501 Fiber Optic Transmitter and MRX8501 Fiber Optic Receiver were proton tested at UCD using 63 MeV protons. The MTX8501 and MTR8501 are 12 channel, high-speed (1.25 Gbps/channel) optical transmitters and receivers, respectively. The transmitter is a 1x12 oxide-confined VCSEL array that emits light with a wavelength of 850 nm. The receiver consists of an array of 12 fast photodiodes (of unknown technology).

Both the transmitter and receiver were mounted on individual evaluation boards that minimize stray capacitances and allow for maximum frequency operation.

The electrical input signal was supplied by a BERT. An attenuator was inserted in the optical path to reduce the light intensity in order to measure the optical power budget. For proton testing, only one of the 15 channels was used. Each run involved a different set of experimental parameters, including angle, attenuation and transmission rate. Two different receivers (photodiodes) and one transmitter were tested. The BER showed an order of magnitude increase when the proton beam was close to grazing incidence. Figure 18 shows the BER as a function of angle.

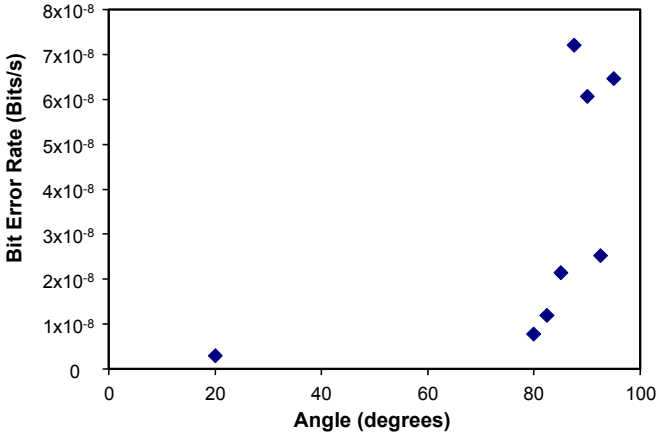

Figure 18. Bit error rate as a function of angle of incidence for a data rate of 1.25 GHz, showing the significant increase at 90 degrees.

The BER was found also to depend on the attenuation setting and the data transmission rate. This suggests that SETs in the detectors can be produced via direct ionization by 63 MeV protons traveling over the long path lengths in the lateral direction of the photodiode. This has previously been observed [32]. No SEEs were observed when the transmitter was irradiated. For more details refer to the full test report [33].

9) Pentium PIII 1200, 1000, 933, 850, and 800 MHz

Pentium III (P3) devices ranging in speed from 550 MHz to 1.2 GHz were tested for SEE. The P3 devices were tested four times for SEE – TAMU with heavy ions in March of 2001, IUCF with protons in May of 2001, TAMU in October 2001 and IUCF in February 2002. Each test added newer generation technology devices and improved software to examine the effects in more detail or to examine unanticipated effects observed in previous tests.

The final testing done at IUCF involved three technology generations (0.25, 0.18, and 0.13 micron) and was done across the entire speed range of 466 MHz to 1.2 GHz (the 466 MHz was achieved by lowering the clock speed on a 700 MHz device). For all SEFI and upset events that were observed, no difference in cross sections were seen between all three generations. However, an interesting piece of data observed in this testing involved the L2 cache (see Figures 19). This data points out a major testing issue that arose during both heavy ion and proton testing. The issue was that when the cache was loaded sequentially (Test C) and was run for the 50 and 25 percent cases, a different per-bit cross section was seen. However, when the cache is loaded non-sequentially (Test I), the three percentage cases do not show the same variation. There is nothing in any Intel documentation that indicates any special data fetching, storages, etc., whenever data is continually fetched sequentially. Even if there was, that would not explain why the 100% case Test C is unaffected by whatever mechanism is in place.

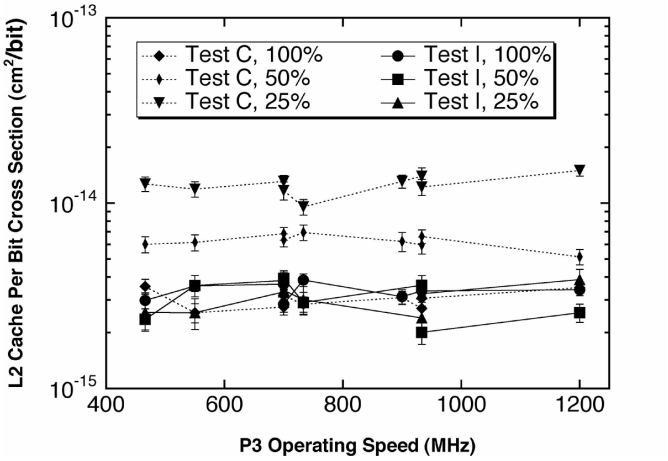

Figure 19: Per Bit L2 Data Cache cross section as a function of P3 operating speed.

Complete test reports are available at the Goddard Radiation Effects & Analysis Group website [34] [35] [36] [37] [38]. A summary paper was presented of the earliest work at the 2001 NSREC Data Work Shop and can be found in that Workshop Record [39]. Additionally, updated presentations and papers (in the respective proceedings) were made at the 2001 MAPLD and 2002 SEE Symposia [40] [41].

V. Single Event Latchup

1) LTC1604, LTC1605, LTC1608

These 16 bit Analog to Digital Converters were tested for SEL. The objective of these tests was to perform a preliminary screening.

- LTC1604 was tested with a 25 MeV/per nucleon Xe beam at TAMU covering a LET range from 40 MeV•cm^2/mg (0 degree) to 65 MeV•cm^2/mg (52 degrees). No SEL events were observed for all angles of incidence up to a fluence of 2x10^6 ions/cm^2.
- LTC1605 was tested with a 15 MeV/ per nucleon Xe beam at TAMU covering a LET range from 54 MeV•cm^2/mg (0 degree incidence) to 60 MeV•cm^2/mg (0 degree incidence, degraded beam). This part showed a very high SEL sensitivity at all LET values. As soon as the beam was turned on the part latches. While the device was latched, the part was not functional. The device recovered its functionality and a normal power supply current after power cycling.
- LTC1608 was tested at BNL using ions with effective LET ranging from 60 MeV•cm^2/mg (Iodine) to 95 MeV•cm^2/mg (Gold at 30 degrees). No SEL event was observed up to an LET of 82 MeV•cm^2/mg (Gold at 0 degree) up to a fluence of 1x10^7 ions/cm^2. One SEL was observed at an LET of 87 MeV•cm^2/mg (Gold at 20 degrees) at a fluence of 7x10^6 ions/cm^2. Two SELs were observed at a LET of 95 MeV•cm^2/mg for a fluence of 8.5x10^6 ions/cm^2. [42] [43] [44]

2) ADG452

The analog switch ADG452 from Analog Devices was tested for SEL at BNL using ions covering a LET range from 60 MeV•cm^2/mg (Iodine at 0 degree) to 82 MeV•cm^2/mg (Gold at 0 degree). No SEL events were observed for all LET values up to a fluence of 1x10^7 ions/cm^2.

3) ICL7662

The voltage converter ICL7662 from Intersil was tested for SEL at BNL at a LET of 82 MeV•cm^2/mg (Gold at 0 degree). No SEL events were observed up to a fluence of 1x10^7 ions/cm^2.

4) XA1

The XA1, an Application Specific Integrated Circuit (ASIC) intended to process data from 128 detector elements, was tested for SEL at TAMU. The ASIC is designed by IDE Assoc. of Norway and fabricated in 1.2 micron feature size bulk CMOS and two different 0.8 micron epitaxial CMOS processes by Austria Mikro Systeme (AMS) International. These devices were tested with a flight project provided set up (to ensure fidelity to the intended application) for susceptibility to heavy-ion and proton induced single-event latchup (SEL). The experimental setup included four separate power supplies that supplied positive and negative biases to the analog and digital portions of the ASIC. For the purposes of this test, a SEL was said to have occurred if any of the power supplies experienced a current spike and the

normal functionality of the part was disrupted. The power supplies were configured so that they could operate either with or without current limiting and power cycling in the event of an SEL.

The Bulk CMOS ASICs were tested at BNL, and the ASICs implemented on epi processes were tested at TAMU. The Bulk CMOS ASICs were found to be susceptible to SEL with an onset LET of about 5 MeV•cm^2/mg and a limiting cross section of about 1x10^{-2} cm^2. The ASICs on epi processes were found to have an onset LET for SEL of 8 MeV•cm^2/mg, with a limiting cross section about a factor of 10 smaller than the bulk process.

To determine whether the SEL mode(s) were destructive, several ASICs were tested without current limiting. No ASICs exhibited any failures up to an LET of 37 MeV•cm^2/mg and a fluence of 1x10^7 particles/cm^2. For LETs above 37, about 3% of the SELs in the bulk ASICs were destructive, perhaps indicating the existence of multiple SEL modes. The ASICs on epi did not exhibit destructive SEL, but due to problems at the cyclotron could only be tested to an LET of 41 MeV•cm^2/mg.

The low onset LETs of the SEL modes suggest that these parts could be susceptible to proton-induced SEL. However, no SELs were observed during tests with 63 MeV protons at the UC Davis proton cyclotron up to the point where the XA1s failed due to TID (1.2-1.8x10^{11} protons/cm^2). Note: The TID degradation did anneal, and the parts were operational by the time they were returned to GSFC.

5) PCA80C522

The Phillips Processor device PCA80C522 was tested for SEE at BNL. Sample size was one part. For each of the test runs, the device was biased with 5 V and run at 16 MHz in the idle mode. For all ions used, single event latchup was observed. Latchup currents measured varied from approximately 13 to 90 mA, where current was approximately 300 uA in the idle mode.

The LET_{th} for latchup is approximately 3-5 MeV•cm^2/mg and the saturation cross section is approximately 3x10^{-3} cm^2 or higher. The "or higher" comment comes from the fact that the data taken at the three highest LET points was limited due to the particle flux rates achievable

The second part of the testing was the dwell test. This data is summarized in Table 12. Dwell times of 5, 10, 15, 30 and 60 seconds were used for this testing. For each of these cases, the latchup current was at whatever level occurred (no effort was made to choose the current level for the dwell testing). For the first four time intervals, the processor after having its power cycled, resumed normal operation. However, after latching and being allowed to stay in the latched state for 60 seconds, a power cycle would not recover the normal operation (current draw stayed in excess of 15 mA). No number of power cycles or power off times were able to recover the DUT to nominal operation. Therefore, the latchup that occurs in these devices does become destructive if allowed to stay latched for a time in excess of 30 seconds.

It should also be noted that numerous events were observed that required a reset to the PCA80C552 rather than a power cycle. These SEFIs were not gathered except to note that they occurred. The device was approximately 5-10 times more sensitive to SEFIs than to latchup. [45]

TABLE 12: SUMMARY OF DWELL TESTING FOR THE PCA80C522

SEL current in mA	Time in seconds of dwell	Recovery?
90	5	yes
58	10	yes
60	15	yes
84	30	yes
26	60	No, hard failure of device

VI. DISPLACEMENT DAMAGE

A. Misc:

1) BAE CCD486

A BAE Systems/Fairchild CCD486 charge-coupled device (CCD) imager was subjected to proton testing at UCD for the Hubble Space Telescope Advanced Camera for Surveys (ACS) program. The CCD486 is a 4k x 4k, full frame, n-channel, 15µ pixel pitch imager with a 3µ supplemental implant (mini-channel) in both the vertical and horizontal registers. The imager was irradiated with 63 MeV protons. Two different regions of the CCD were exposed to fluences of 2.5x10^9 p/cm^2 and 5x10^9 p/cm^2 using a moveable metal mask. The irradiations were carried out at room temperature with the imager unbiased. Pre- and post-rad characterization was performed in the Ball Aerospace and Technologies Corporation ACS CCD characterization facility. Parallel First Pixel Response (FPR) CTE measurements taken at –81°C exhibited simple power law behavior as a function of signal level except for a slight change in the slope of the 5x10^9 p/cm^2 curve at low signal levels. As in previous studies, FPR was found to be in good agreement with ^{55}Fe measurements at a signal level of 1620 electrons. Serial FPR measurements for the 2.5x10^9 p/cm^2 half of the imager showed a bump in the CTE curve at high signal levels that resulted in a decrease in CTE (or an increase in CTI). The CTE and CTI measurements are shown in Figures 20 and 21, respectively.

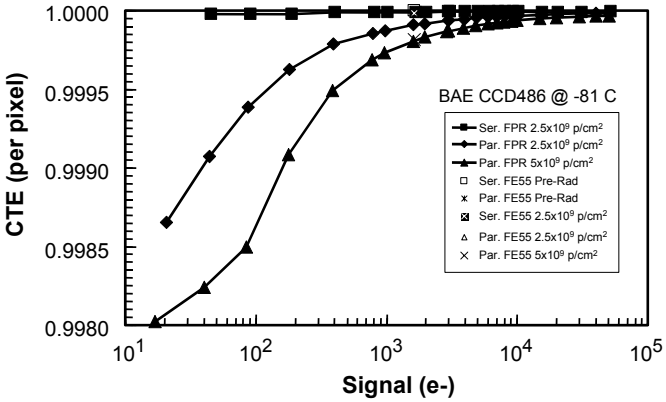

Figure 20: BAE CCD486 CTE radiation test results.

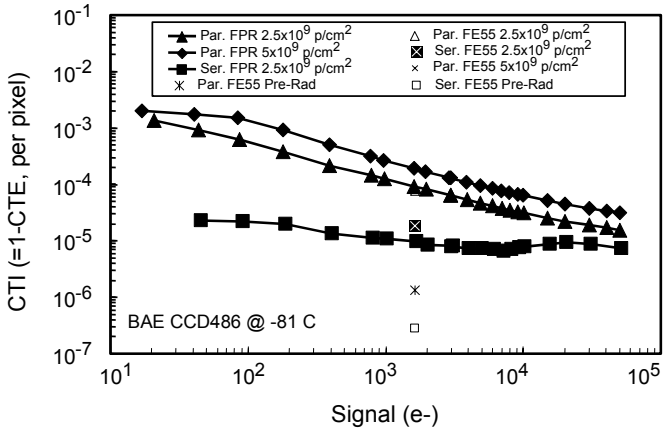

Figure 21: BAE CCD486 CTI radiation test results.

We interpret the bump as an indication that the signal packet, confined in the horizontal register mini-channel at low signal levels, reached the overflow capacity of the mini-channel. The decrease in CTE was caused by the increase in the signal packet volume as the charge expanded beyond the edge of the mini-channel. We speculate that a similar CTE characteristic did not occur in the vertical register because the vertical shift rate is much slower than the horizontal shift rate. For this test, the serial shift rate was 22 µsec/pixel and the vertical shift rate was 91 msec/row. The much slower vertical shift rate may have allowed carriers confined in the mini-channel time to escape into the main channel before the charge packet is transferred into the next pixel. [46]

2) TIL25

The Texas Instruments TIL25 single-heterojunction P-N GaAs LED was tested for proton damage at UCD. Two samples were tested (SN3 and SN4). The measured output power (P) for each LED at each fluence level is normalized to the pre-irradiation output power (P_o). Figure 22 shows the degradation (P/P_o) of both LEDs at each exposure level (fluence) when V_{IN}=3.3V and I_F=35mA. There was a significant amount of degradation seen in both of devices after receiving a total fluence of $2.56x10^{10}p/cm^2$. Following the final step (total fluence is $1.53x10^{11}p/cm^2$), the device performance had degraded significantly, to less than 15% of its initial value. This degradation curve is typical of a single heterojunction LED. [47] [48]

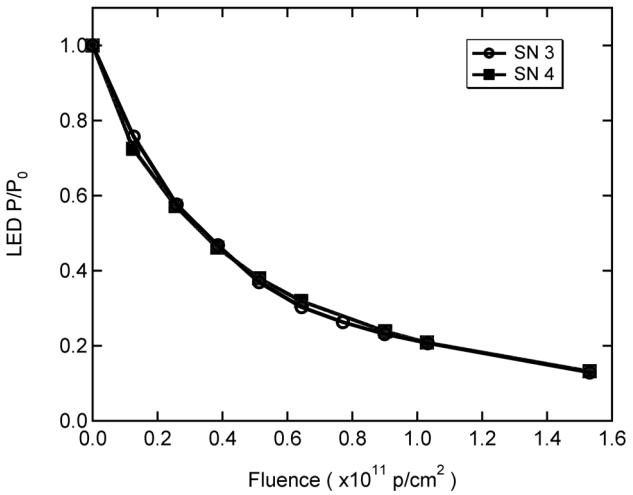

Figure 22. Proton induced degradation of LED power output for both TIL25 devices. The LED output power was normalized to the pre-radiation values.

3) TIL601

The Texas Instruments TIL601 an N-P-N planar silicon phototransistor was tested for proton damage at UCD. Two samples were tested (SN3 and SN4). The devices were exposed to protons at UCD. The phototransistor output current (I) was monitored for radiation-induced degradation at various fluence levels. The current (I) was measured across the load R2 following the phototransistor at each fluence level and was normalized to the pre-irradiation current (I_o). Figure 23 shows the degradation (I/I_o) of both phototransistors at each exposure level (fluence) when V_{CC}=5.0V. There was a significant amount of degradation seen in both devices after $6.4x10^{10}p/cm^2$. Following the final step (total fluence of $1.53x10^{11}p/cm^2$), the device performance had degraded significantly, to less than 30% of its initial value. [49]

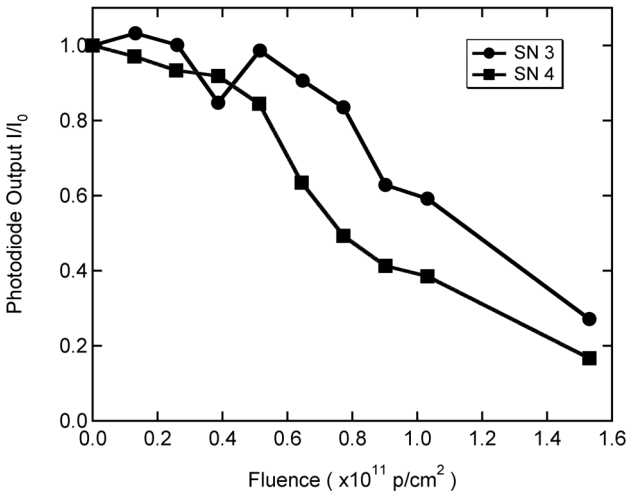

Figure 23. Proton induced degradation of the current for both TIL601 phototransistors. The photodiode current was normalized to the pre-radiation values.

4) 4N49

Three samples of Micropac 4N49 optocouplers containing a single-heterojunction GaAs LED and an N-P-N planar silicon phototransistor were tested with protons at UCD. The purpose of this test was to provide upper and lower bounds for the degradation of the parameter V_{CE} in the Micropac 4N49 optocoupler devices (LDCs 9803 and 9818).

The DUTs were irradiated unbiased with 63MeV protons and then tested after each step by sweeping through various V_{IN} and V_{CC} values to determine the change in V_{CE} for those conditions. The devices were operated with a custom setup through a GPIB controller and a laptop. V_{CC} was swept from 22V to 34V in 1V steps with V_{IN} held constant for each V_{IN} value. V_{IN} values ranged from 3.6V to 5.1V in 0.1V increments. The total number of measurements per DUT per run was 208. In all, six step irradiations were performed on the samples.

The project that this was tested for gave the following conditions as input test parameter bounds: $V_{CC\ MIN}$ = 24V, $V_{CC\ Nom}$ = 28V, $V_{CC\ MAX}$ = 34V, and $V_{IN\ MIN}$ = 3.6V, $V_{IN\ Nom}$ = 4.5V, $V_{IN\ MAX}$ = 5.1V. The resulting V_{CE} is the test result of interest for the project. For the purposes of presenting results in an interpretable manner, V_{CE} is presented at the maximum, nominal and minimum values for V_{CC} and V_{IN} (in all 9 combinations) in order to bound the range of V_{CE}. At $1x10^{11}p/cm^2$, V_{IN} is the driving factor in greater than acceptable V_{CE} values. In order for the device to remain within specifications, higher V_{IN} values would be preferred. Table 13 gives the average V_{CE} for the devices' worst, nominal and best cases. [50]

TABLE 13: 4N49 SUMMARY TABLE:

	V_{CC}	V_{IN}	Initial V_{CE}	Avg. V_{CE} at proton fluence of $1x10^{10}$	Avg. V_{CE} at proton fluence of $3x10^{10}$	Avg. V_{CE} at proton fluence of $5x10^{10}$
Worst Case	34V	3.6V	0.136 ±0.006V	0.158 ±0.004V	0.199 ±0.005V	0.273 ±0.002V
Nominal	28V	4.5V	0.116 ±0.005V	0.134 ±0.003V	0.166 ±0.003V	0.204 ±0.003V
Best Case	24V	5.1V	0.104 ±0.004V	0.121 ±0.003V	0.149 ±0.002V	0.182 ±0.002V

VII. TOTAL IONIZING DOSE (TID)

A. ADCs:

1) AD7714

The 24 bit ADC AD7714 from Analog Devices was tested to a total dose of 20 krad(Si) at a dose rate of 0.86 rad/s. Tests were performed at NAVSEA/CRANE laboratories. Two devices were statically biased, three were dynamically biased. Results of the total dose testing indicate:

- Both devices biased statically and all three devices biased dynamically failed and became non-functional between 10 krad(Si) and 20 krad(Si).
- Both devices biased statically and all three devices biased dynamically began showing degradation between 7.5 krad(Si) and 20 krad(Si) as evidenced by increasing power supply currents. Figure 24 shows the degradation versus dose of the standby current.
- Both devices biased statically and all three devices biased dynamically performed to specified effective resolution of greater than 17 bits up to 10 krad(Si).
- Both devices biased statically and all three devices biased dynamically showed no degradation in integral nonlinearity up to 10 krad(Si).
- After the 168 hour biased room temperature anneal, all five devices remained nonfunctional. [51]

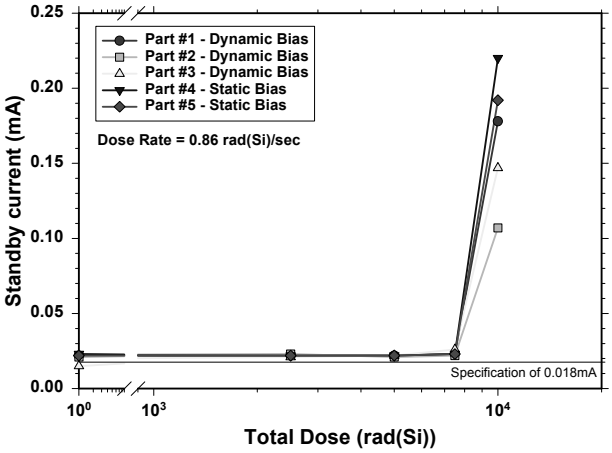

Figure 24: AD7714 degradation of the standby current verus total dose.

2) LTC1272

The 12 bit ADC LTC1272 from Linear Technology was tested to a total dose up to a dose of 30 krad(Si) at a dose rate of 0.83 rad/s. Tests have been performed at NAVSEA/CRANE laboratories. Two parts were statically biased, six dynamically biased. Results of the total dose testing indicate:

- Both devices biased statically and one device biased dynamically had missing codes at 7.5krad(Si).
- Both devices biased statically showed degradation in effective number of bits at 7.5krad(Si). Three devices biased dynamically showed degradation in effective number of bits at 7.5krad(Si).
- Both devices biased statically had (maximum) differential non-linearity (DNL) greater than +1.0 (specification limit) at 5krad(Si). Five devices biased dynamically had (maximum) DNL greater than 1.0 at 7.5krad(Si). See figure 25.
- Parametric shifts were observed at 5krad(Si).
- All eight devices were still functional, though at a significantly degraded performance level, at 30krad(Si) See figure 26.
- After a 168-hour biased room temperature anneal, all eight devices showed a significant improvement in performance, but did not improve to pre rad levels. [52]

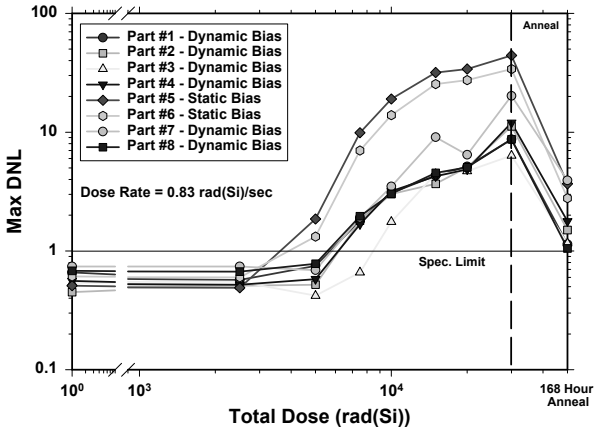

Figure 25: LTC1272 degradation of the differential non linearity versus dose.

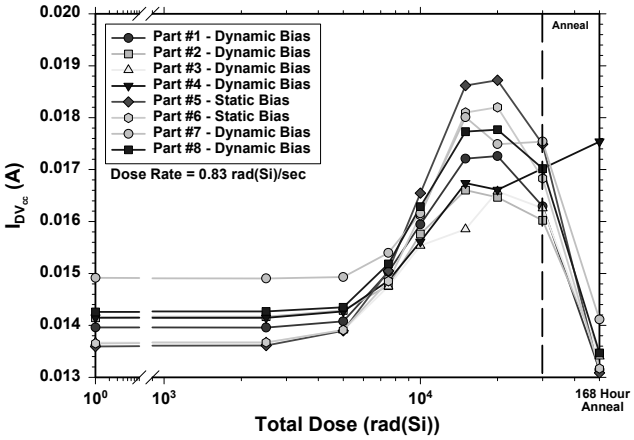

Figure 26: LTC1272 degradation of the differential supply current versus dose

3) AD6640

NAVSEA Crane Division performed total dose testing on five Analog Devices AD6640, 12 bit ADC's. Three parts were tested with a static bias applied during irradiation and two parts were tested with a dynamic bias applied. Static bias devices were irradiated with nominal DC power applied and the clock, and all other inputs grounded. Dynamically biased parts used the same nominal DC power as the static bias condition, a 62.5 MHz Encode clock signal and a 1 MHz, 1.7 V peak-to-peak amplitude sinusoidal input signal.

The AD6640 experienced no functional or parametric failures up to 30 krad(Si). Two AD6640s were tested to 100 krad(Si) and no functional or parametric failures were observed. No significant changes in aperture uncertainty jitter were noted up to 30 krad(Si), nor for the two devices tested up to 100krad(Si). [53]

B. Power MOSFETs:

1) FDN361AN

The FDN361AN 30V 0.15 ohms N channel MOSFET transistor from Fairchild was tested to total dose up to a dose of 50 krad at a dose rate < 1 rad/s. Tests were performed at NAVSEA/CRANE laboratories. Test results indicated that IDSS increased to a maximum of 32 uA at 50 krds and decreased to 17 uA after anneal; RDSON decreased slightly to a minimum of 0.1 ohms at 50 krds and to 0.098 ohms after anneal; and VGSTH decreased to a minimum of 0.23 V at 50 krds and to 0.28 V after anneal. The degradation versus dose of the threshold voltage is shown in Figure 27. [54]

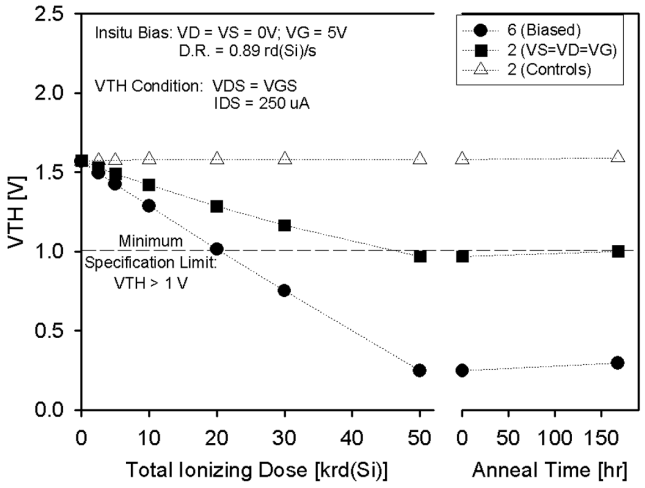

Figure 27: FDN361AN degradation of threshold voltage versus dose.

2) NDS352A

The NDS352A 30V 0.5 ohms P channel MOSFET transistor from Fairchild was tested for dose up to 50 krad(Si) at a dose rate < 1 rad/s. Tests have been performed at NAVSEA/CRANE laboratories. Test results indicated that IDSS increased to a maximum of 522 pA at 50 krds and to 575 pA after the anneal; RDSON increased to a maximum of 0.98 ohms at 50 krads(Si) and to 0.91 ohms after the annealing; and VGSTH increased to a maximum of -2.63 V at 50 krds and to -2.61 V after the annealing. [55]

3) IRLML2803

The IRLML2803 30V 0.25 ohms N channel MOSFET transistor from International Rectifier was tested to a total dose of 50 krad(Si) at a dose rate < 1 rad/s. Tests were performed at NAVSEA/CRANE laboratories. Test results indicated that IDSS increased to a maximum of 442 nA at 50 krads(Si) and to 10.8 nA after annealing; RDSON decreased slightly to a minimum of 0.23 ohms at 50 krds but increased slightly to 0.29 ohms after annealing; and VGSTH decreased to a minimum of 0.67 V at 50 krads(Si) and to 1.15 V after annealing. The degradation versus dose of the threshold voltage is shown in Figure 28. [56]

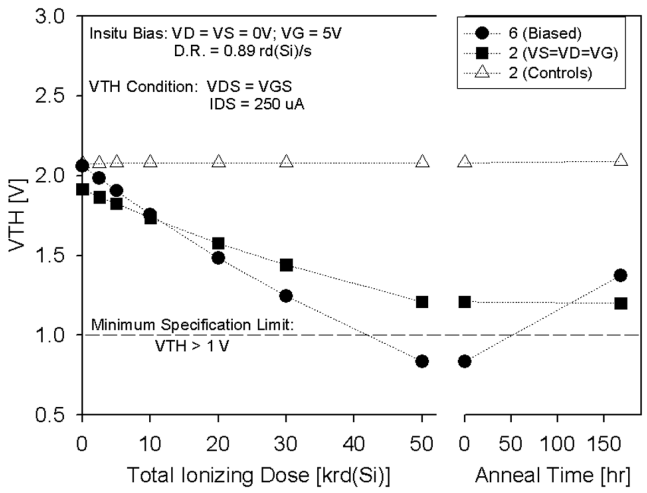

Figure 28: IRLML2803 degradation of threshold voltage versus dose

4) IRLML5103A

The IRLML5103A 30V 0.6 ohms P channel MOSFET transistor from International Rectifier was tested up to a dose of 50 krad(Si) at a dose rate < 1 rad/s. Tests were performed at NAVSEA/CRANE laboratories. Test results indicate that IDSS increased to a maximum of 240 pA at 50 krads(Si) and to 555 pA after the anneal; RDSON increased to a maximum of 55 ohms at 50 krads(Si) and to 54 ohms after the annealing; and VGSTH increased to a maximum of -3.15 V at 50 krds and to -3.14 V after the annealing. [57]

5) 2N5114

The 2N5114 40V P channel JFET transistor was tested to a total dose of 50 krad(Si) at a dose rate < 1 rad/s. Tests were performed at NAVSEA/CRANE laboratories. Test results indicated that only IDSS and IGSS were sensitive to total ionizing dose effects up to 50 krad(Si). Both of these parameters exceeded their specification limit at 50 krad(Si). The bias condition that produced the largest change was VD=VS=VG=0 volts. IDSS increased from 5.2 to 555 pA at 50 krad(Si) and to 584 pA after annealing. IGSS increased from 8.5 to 994 pA at 50 krad(Si) and to 1080 pA after annealing. RDS_ON slightly increased from 60 to 62 ohms at 50 krad(Si) and after anneal. VGS_OFF increased from 7.70 to 7.75 V at 50 krads(Si) and to 7.85 V after annealing. [58]

C. Miscellaneous Devices:

1) Intel Pentium III

Intel Pentium III (P3) processors, ranging from 550 MHz to 1.0 GHz, were exposed to the total dose environment at the IUCF proton facility (as part of proton SEE testing) and to Cobalt-60 gamma rays at the GSFC-REF. It should be noted that the DUTs rated at 550 MHz are 0.25 µm technology, while all other DUTs tested are 0.18 µm technology. The parts in unbiased and biased states tested at IUCF were exposed to proton doses with various increments up to approximately 100 krads(Si). After each dose, all parts passed all functional tests and the monitored voltages and currents did not change. No parametric timing measurements were done in these tests. These timing tests would be expected to be more sensitive to dose. The parts, however, did not degrade in timing sufficiently to fail any of the functional tests that were performed.

Total dose testing using the Cobalt-60 source at GSFC was stopped due to the GSFC-REF shutting down for maintenance. Several P3 devices, in an unbiased condition, were exposed to various doses, one in excess of 3700 krads(Si). They showed little sign of degradation in either supply currents or timing and functionality testing. One biased Pentium III DUT did functionally fail after exposure to an approximate dose of 511 krads(Si). A replacement part was tested under bias, and had exceeded a dose of 573 krads(Si) when it was removed due to funding constraints. All devices tested, besides the failure at 511 krads(Si), were never observed to have functional failure. Complete details of the parts tested and the test results can be found in "Total Ionizing Dose Testing of the Intel Pentium III (P3) and AMD K7 Microprocessors," [59]

2) AD8151

During proton SEE testing (described previously), the Analog Devices AD8151 was exposed to doses up to 168 krads(Si) at UCD. Performance degradation was noticed at about 70 krads(Si), and the operating current continued to increase up to 168 krads(Si). At the latter dose, repeated adjustment of the delay window was necessary to maintain error-free operation in the absence of radiation. However, the part remained functional. [28] [29]

VIII. Summary

We have presented recent data from SEE, and proton-induced damage tests on a variety of mainly commercial devices. It is the authors' recommendation that this data be used with caution. We also highly recommend that lot testing be performed on any suspect or commercial device.

IX. Acknowledgment

The Authors would like to acknowledge the sponsors of this effort: NASA Electronics Radiation Characterization (ERC) Project, a portion of NASA Electronic Parts and Packaging Program (NEPP), NASA Flight Projects, NASA Remote Exploration and Experimentation (REE) Project, and the Defense Threat Reduction Agency (DTRA) under IACRO 02-4039I.

X. References

[1] NASA/GSFC Radiation Effects and Analysis home page, http://radhome.gsfc.nasa.gov

[2] Department of Defense Test Method Microcircuits, MIL-STD-883 Test Method Standard, Microcircuits, MIL-STD-883 (1000's) (Complete) 6-section text, 1000 series test methods, (With all Notices included in Main Document) Dated: 18 December 2000, File name: std883inc-1000.pdf, File size: 1414 kb, pp112-121, http://www.dscc.dla.mil/Programs/MilSpec/ListDocs.asp?BasicDoc=MIL-STD-883, December 1996.

[3] C. Poivey, et al., " Development of a test methodology for single event transients (SET) in lnear devices," IEEE Trans. Nucl. Sci., vol. 48, pp. 2180-2186, December 2001.

[4] S. Buchner, et al., "Single-event transient characterization of LM119 voltage comparator," http://radhome.gsfc.nasa.gov/radhome/papers/B122101_paper_LM119.pdf, December 2001.

[5] S. Buchner, et al., "Test report: single-event transient characterization of LM119 voltage comparator," http://radhome.gsfc.nasa.gov/radhome/papers/B122101_LM119.pdf, December 2001.

[6] C. Seidleck et al., "Test methodology for characterizing the SEE sensitivity of a commercial IEEE 1394 serial bus (FireWire)," NSREC02_PI-3 accepted for publication in IEEE Trans. Nucl. Sci., December 2002.

[7] J.W. Howard et al., "Proton Single Event Effects (SEE) Testing of the Myrinet Crossbar Switch and Network Interface Card," NSREC02_W-8 accepted for publication in IEEE NSREC 2002 Data Workshop, July, 2002.

[8] P.W. Marshall, W.B. Byers, C. Conger, E.S. Eid, G. Gee, M.R. Jones, C.J. Marshall, and R.A. Reed, "Heavy Ion Transient Characterization of a Photobit Hardened-by-Design Active Pixel Sensor Array," accepted for publication in IEEE NSREC 2002 Data Workshop, July, 2002.

[9] R. A. Reed, P.W. Marshall, H. Ainspan, C.J. Marshall, and H.S. Kim, "Single event upset test results on a prescalar fabricated in IBM's 5HP silicon germanium heterojuction bipolar transistors BiCMOS technology," IEEE NSREC 2001 Data Workshop, pp. 172-176, July, 2001.

[10] R.A. Reed, P.W. Marshall, P.J. McNulty, B. Fodness, H. Kim, R. Reedy, G. Wuo, J. Swonger, C. Tabbert, S. Buchner, and K. LaBel "Effects of proton beam angle-of-incidence on singel-event upset cross-section measurements," accepted for publication in IEEE Trans. Nucl. Sci., December 2002.

[11] K. A. LaBel, et al., "Single event transients in LM124 operational amplifier laser test report," http://radhome.gsfc.nasa.gov/radhome/papers/NRL01MAY_LM124.pdf, May 2001.

[12] S. Kniffin et al., 'Heavy ion single event effects test results for three candidate 22V10 reprogrammable logic devices," http://radhome.gsfc.nasa.gov/radhome/papers/B030402_22V10.pdf, March 2002

[13] A. Sanders, et al., "Heavy ion single event effects test results for Anadigm AN10E40 field programmable analog array (FPAA)," http://radhome.gsfc.nasa.gov/radhome/papers/B030402_AN10E40.pdf, March 2002

[14] J. Howard, et al., " Single event transient and destructive single event effects re-testing of the MDI3051RES05ZF Modular Devices, Inc. DC/DC converters (with radiation hardened MOSFET)," http://radhome.gsfc.nasa.gov/radhome/papers/T100115_MDI05.pdf, October 2001

[15] J. Howard, et al., " Single event transient and destructive single event effects re-testing of the MDI3051RED12ZF Modular Devices, Inc. DC/DC converters (with radiation hardened MOSFET)," http://radhome.gsfc.nasa.gov/radhome/papers/T100115_MDI12.pdf, October 2001

[16] J. Howard, et al., "Single event transient and destructive single event effects re-testing of the MDI3051RED15ZF Modular Devices, Inc. DC/DC converters (with radiation hardened MOSFET)," http://radhome.gsfc.nasa.gov/radhome/papers/T100115_MDI15.pdf, October 2001

[17] C. Poivey, and Z. Kahric, "Heavy ion single event effects test of switching regulator LM2651 from National Semiconductor," http://radhome.gsfc.nasa.gov/radhome/papers/B030302_LM2651.pdf, March 2002

[18] C. Poivey, et al., "Heavy ion single event effects test of 4A adjustable switching regulator MSK5042 from M. S. Kennedy," http://radhome.gsfc.nasa.gov/radhome/papers/B030302_MSK5042.pdf, March 2002

[19] C. Poivey, et al., Heavy ion single event effects test of power on reset LP3470 from National Semiconductor," http://radhome.gsfc.nasa.gov/radhome/papers/B030302_LP3470.pdf, March 2002

[20] R. Koga, et al., "Techniques of microprocessor testing and SEU-rate prediction," IEEE Trans. Nucl. Sci., vol. NS-32, pp. 4219-4224, December 1985.

[21] C. Poivey et al., "Heavy ion single event effects test of 8 bits ADC AD7821 from Analog Devices 12 bits ADC AD9223 from Analog Devices 12 bits ADC LTC1272 from Linear Technology," http://radhome.gsfc.nasa.gov/radhome/papers/T080101_ADC.pdf, August 2001.

[22] C. Poivey, and J. Forney, "Heavy ion single event effects test of 16 bits DAC LTC1657 from Linear Technology," http://radhome.gsfc.nasa.gov/radhome/papers/B030302_LTC1657.pdf, March 2002.

[23] C. Poivey et al., "Heavy ion single event effects test of 8 bits ADC AD1175 from National Semiconductor," http://radhome.gsfc.nasa.gov/radhome/papers/B030302_ADC1175.pdf, March 2002.

[24] H.S. Kim, C. Seidleck, P. Marshall, and K.A. LaBel, "Single Event Effect Test Report on IEEE 1394 Testing at Brookhaven National Laboratories and TRIUMF," http://radhome.gsfc.nasa.gov/radhome/papers/B062501_1394.pdf, June 2001.

[25] H. Kim et al., "Single-event effects test report on IEEE 1394," http://radhome.gsfc.nasa.gov/radhome/papers/T101401_1394.pdf, October 2001.

[26] J. Howard et al., "Proton Single Event Effects (SEE) Testing of the Myrinet Crossbar Switch and Network Interface Card," http://radhome.gsfc.nasa.gov/radhome/papers/D112601_Myrinet.pdf, November 2001.

[27] S. Buchner, J. Howard, M. Carts, and K. Label, "Single-Event Testing of the AD8151 Digital Crosspoint Switch," submitted for publication in IEEE Trans. Nucl. Sci., December 2002.

[28] P.W. Marshall, M. Carts and S. Buchner, "Proton Testing of the AD8151 Cross-Point Switch," http://radhome.gsfc.nasa.gov/radhome/papers/D013102_AD8151.pdf, January 2002.

[29] J. Howard, M. Carts, and S. Buchner, "Heavy-Ion Testing of the AD8151 Cross-Point Switch," http://radhome.gsfc.nasa.gov/radhome/papers/T031502_AD8151_paper.pdf, March 2002.

[30] H. Becker, "Latent damage form single event latchup," 2002 SEE symposium, Thirteeneth Biennial Single-Event-Effects (SEE) Symposium Proceedings CD, April 2002.

[31] Scott Kniffin, Zoran Kahric, and Hak Kim, "Heavy Ion Single Event Effects Test Results for Agere LSP2916 16-Channel, High Voltage Driver (MEMS)," http://radhome.gsfc.nasa.gov/radhome/papers/B122001_LSP2916.pdf, December 2001.

[32] K.A. LaBel, P. Marshall, C.J. Marshall, M.D'Ordine, M. Carts, G. Lum, H.S. Kim. C.M. Seidleck, T. Powell, R. Abbott, J. Barth, and E.G. Stassinopolous, "Proton induced transients in optocouplers: In-fight anomalies, ground irradiation test, mitigation and implications," IEEE Trans. Nucl. Sci., Vol. 44, No. 6, pp 1885-1892, 1997.

[33] P. Marshall, M. Carts, and S. Buchner, "Proton Testing Emcore MTX8501/MRX8501," http://radhome.gsfc.nasa.gov/radhome/papers/D020102_Emcore.pdf, February 2002.

[34] J. Howard, K. LaBel, M. Carts, R. Stattel, C. Rogers, and T. Irwin, "Proton single event effects testing of the Intel Pentium III (P3) microprocessors," http://radhome.gsfc.nasa.gov/radhome/papers/IU0501.pdf, May 2001.

[35] J. Howard, K. LaBel, M. Carts, R. Stattel, C. Rogers, and T. Irwin, "Heavy ion single event effects testing of the Intel Pentium III (P3) and AMD K7 microprocessors," http://radhome.gsfc.nasa.gov/radhome/papers/TAMU0301.pdf, March 2001.

[36] J. Howard, K. LaBel, M. Carts, R. Stattel, C. Rogers, and T. Irwin, "Heavy ion single event effects testing of the Intel Pentium III (P3) microprocessor," http://radhome.gsfc.nasa.gov/radhome/papers/T101201_P3.pdf, October, 2001.

[37] J. Howard, E. Webb, K. LaBel, M. Carts, R. Stattel, and C. Rogers, "Proton dose and single event effects testing of the Intel Pentium III (P3) and AMD K7 microprocessors," http://radhome.gsfc.nasa.gov/radhome/papers/IU0600.pdf, June 2000.

[38] J. Howard, K. LaBel, M. Carts, R. Stattel, and C. Rogers, "Single event effects testing of the Intel Pentium III (P3) and AMD K7 microprocessors," http://radhome.gsfc.nasa.gov/radhome/papers/IU1200.pdf, December 2000.

[39] J.W. Howard, M.A. Carts, R.Stattel, C.E. Rogers, T.L. Irwin, C. Dunsmore, J.A. Sciarini, and K.A. LaBel, "Total dose and single event ettects testing of the Intel Pentium III (P3) and AMD K7 microprocessors," NSREC01_W7.pdf, IEEE NSREC 2001 Data Workshop, pp. 38-47, July, 2001.

[40] J.W. Howard, M.A. Carts, K.A. LaBel, T.L. Irwin, J.A. Sciarini, and C. Dunsmore, "Update to total dose and single event effects testing of the Intel Pentium III (P3) and AMD K7 microprocessors," MAPLD01_P3.pdf, 2001 MAPLD International Conference Proceedings CD, September 2001.

[41] J. Howard, K. LaBel, M. Carts, R. Stattel, C. Rogers, and T.L. Irwin, "Single event effects testing of the Intel Pentium III (P3) microprocessor," Seesym02_P3.pdf, Thirteeneth Biennial Single-Event-Effects (SEE) Symposium Proceedings CD, April 2002.

[42] C. Poivey, and C. Palor, "Preliminary heavy ion single event effects test of ADC 16 bits LTC1604 from Linear Technology," http://radhome.gsfc.nasa.gov/radhome/papers/T080101_LTC1604.pdf, August 2001.

[43] C. Poivey, C. Palor, and J. Howard, "Preliminary heavy ion single event effects test of ADC 16 bits LTC1605 from Linear Technology," http://radhome.gsfc.nasa.gov/radhome/papers/T100101_LTC1605.pdf, October 2001.

[44] C. Poivey, S. Kniffin, and C. Palor, "Preliminary heavy ion single event effects test of ADC 16 bits LTC1608 from Linear Technology," http://radhome.gsfc.nasa.gov/radhome/papers/B030302_LTC1608.pdf, March 2002.

[45] J. Howard, K. LaBel, J. Forney, and H. Kim, "Single event latchup testing of the PCA80C552 Phillips Processor," http://radhome.gsfc.nasa.gov/radhome/papers/B082301_PCA80C552.pdf, August 2001.

[46] M.R. Jones, R. Schrein, W. Koldewyn, M. Sirianni, P. Vu, and P.W. Marshall, "BAE Systems Charge Coupled Device Radiation Test Results," http://radhome.gsfc.nasa.gov/radhome/papers/D030901_CCD486.pdf, March 2001.

[47] R. A. Reed, et al., "Energy Dependence of Proton Damage in AlGaAs Light-Emitting Diodes," IEEE Trans. Nucl. Sci., Vol. 47, pp 2492-2499, December 2000.

[48] J. Howard, R. Reed, S. Kniffin, H. Kim, and P. Marshall, "Proton displacement testing of the TIL 25 LED," http://radhome.gsfc.nasa.gov/radhome/papers/D040101_TIL25.pdf, April 2001.

[49] J. Howard, R. Reed, S. Kniffin, H. Kim, and P. Marshall, "Proton displacement testing of the TIL601 phototransistor," http://radhome.gsfc.nasa.gov/radhome/papers/D040101_TIL601.pdf, April 2001.

[50] S. Kniffin, P. Marshall, and H. Kim, "Report for VCE Degradation in Mii 4N49 Optocouplers for IRAC," http://radhome.gsfc.nasa.gov/radhome/papers/D050101_4N49.pdf, May 2001.

[51] J.P. Bings, "NAVSEA AD7714YRU Total Dose Test Report," http://radhome.gsfc.nasa.gov/radhome/papers/N032902_AD7714.pdf, March 2002.

[52] J.P. Bings, "NAVSEA LTC1272 total dose test report," http://radhome.gsfc.nasa.gov/radhome/papers/N121901_LTC1272.pdf, December 2001.

[53] J.P. Bings, "NAVSEA AD6640 total dose test report," http://radhome.gsfc.nasa.gov/radhome/papers/N103001_AD6640.pdf, October, 2001.

[54] J. Titus, "NAVSEA Crane radiation test report no: NSWC C6054-FDN361AN-0001," http://radhome.gsfc.nasa.gov/radhome/papers/N123101_FDN361AN.pdf, December 2001.

[55] J. Titus, "NAVSEA Crane radiation test report no: NSWC C6054-NDS352AP-0001," http://radhome.gsfc.nasa.gov/radhome/papers/N123101_NDS352A.pdf, December 2001.

[56] J. Titus, "NAVSEA Crane radiation test report no: NSWC C6054-IRLML2803-0001," http://radhome.gsfc.nasa.gov/radhome/papers/N123101_IRLML2803.pdf, December 2001.

[57] J. Titus, "NAVSEA Crane radiation test report no: NSWC C6054-IRLML5103-0001," http://radhome.gsfc.nasa.gov/radhome/papers/N123101_IRLML5103A.pdf, December 2001.

[58] J. Titus, "NAVSEA Crane radiation test report no: NSWC C6054-2N5114-0001," http://radhome.gsfc.nasa.gov/radhome/papers/N013102_2N5114.pdf, January 2002.

[59] J. Howard, K. LaBel, M. Carts, R. Stattel, C. Rogers, T. Irwin and Z. Kahric, "Total Ionizing Dose Testing of the Intel Pentium III (P3) and AMD K7 Microprocessors," http://radhome.gsfc.nasa.gov/radhome/papers/G020802_P3_TID.pdf, February 2002.